PANDA

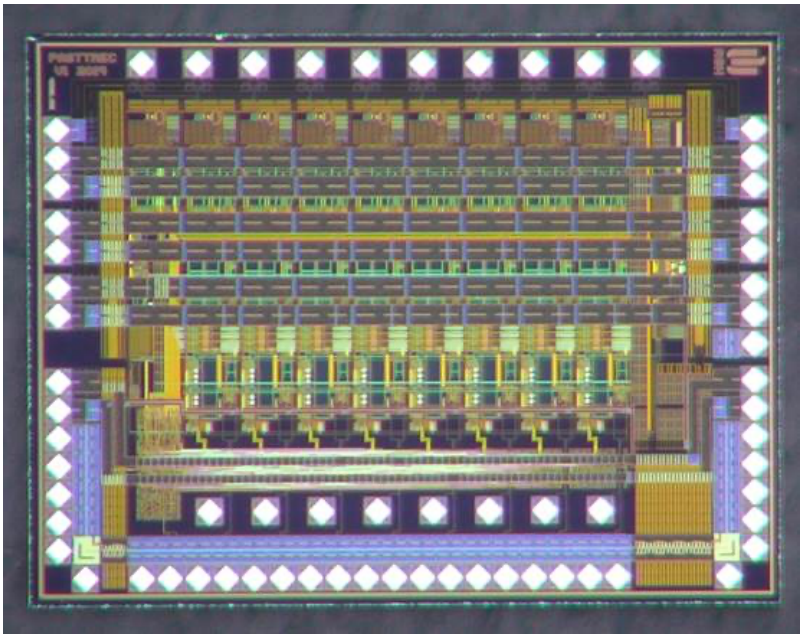

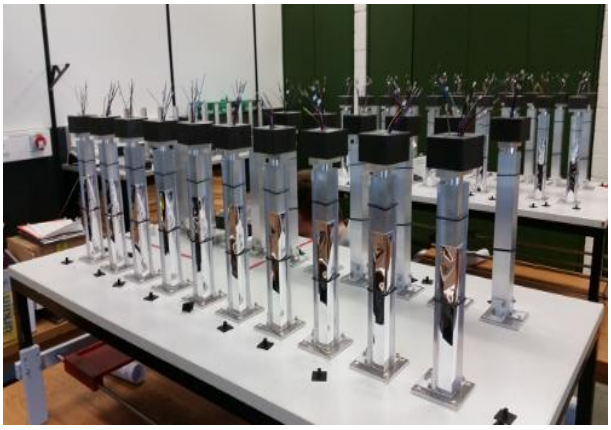

Annual Report

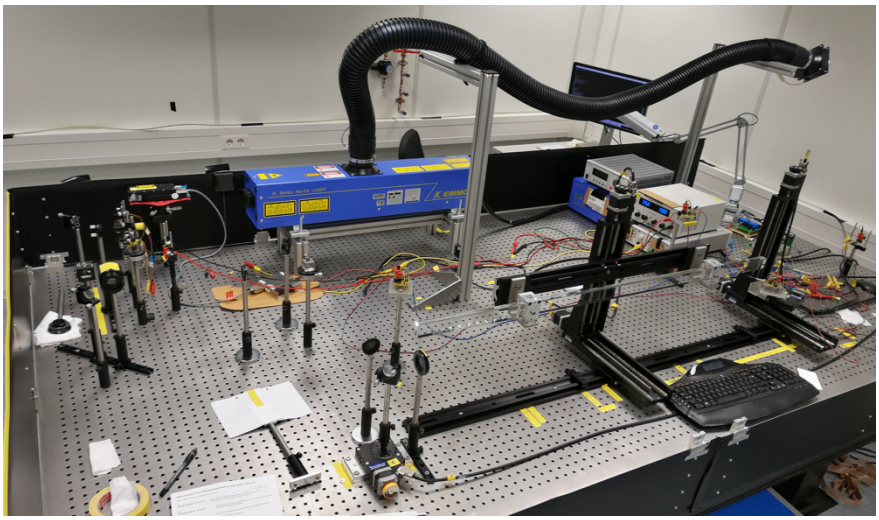

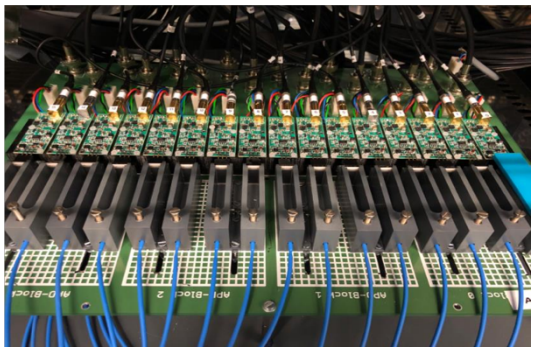

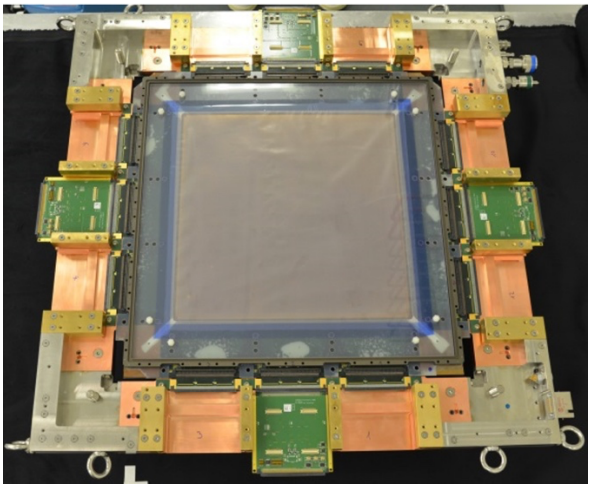

2019

65 Institutes

Università Politecnica delle Marche, Ancona
University Basel
Institute of High Energy Physics (IHEP), Beijing
Ruhr-University Bochum
Abant Izzet Baysal University Golkoy, Bolu
Rheinische Fridrich-Wilhelms-University Bonn
Università degli Studi di Brescia
AGH University of Science and Technology, Cracow
IFJ PAN, Cracow
Jagiellonian University, Cracow
Cracow University of Technology
FAIR, Darmstadt
GSI Helmholtzcentre for Heavy Ion Research, Darmstadt
Joint Institute for Nuclear Research (JINR), Dubna
Friedrich-Alexander-Universität Erlangen-Nürnberg
Northwestern University, Evanston
Goethe-University Frankfurt
Laboratori Nazionali di Frascati (LNF)
University & INFN Genova
Justus Liebig-University Giessen
Giresun University
Glasgow University
KVI-CART, Groningen
Gauhati University, Guwahati
USTC Hefei
URZ Heidelberg
Doğuş University, Istanbul
Okun University, Istanbul
Forschungszentrum Jülich
Institute of Modern Physics (IMP), Lanzhou
Laboratori Nazionali di Legnaro (LNL)
Lund University
Helmholtz-Institute Mainz
Gutenberg-University Mainz
Horia Hulubei National Institute for R&D in Physics and Nuclear Engineering (IFIN-HH), Magurele
Institute for Nuclear Problems (INP), Minsk
NRC "Kurchatov Institute" - ITEP Moscow
Moscow Power Engineering Institute
Westfälische Wilhelms-Universität Münster
Suranaree University of Technology (SUT), Nakhon Ratchisma
Budker Institue for Nuclear Physics, Novosibirsk
Novosibirsk State University (NSU)
INP Orsay
University of Wisconsin, Oshkosh
University & INFN Pavia
Petersburg Nuclear Physics Institute
West Bohemian University, Pilzen
Charles University, Prague
Czech Technical University, Prague
Institute of High Energy Physics (IHEP), Protvino
IRFU CEA-Saclay
KTH Stockholm
Stockholm University
Sardar Vallabhbhai National Institute of Technology (SVNIT), Surat
Veer Narmad South Gujarat University, Surat
Florida State University Tallahassee
Nankai University, Tianjin
University & INFN Torino
Politecnico di Torino
University Trieste
Uppsala University
Stefan Meyer-Institute (SMI), Vienna
National Center for Nuclear Research (NCBJ), Warsaw and
York University

from 18 Countries

Preface

Apart from a lot of progress to get the remaining TDRs ready, submitted and approved, the Phase-0 activities have taken up a lot of momentum and the construction for Phase-1 progressed as well as work on the Phase-1 physics paper. More about this is mentioned in the respective chapters of this annual report.

In addition, Networking and attracting more and new scientists to PANDA has been a major issue. In that respect a couple of events have taken place over the year 2019.

End of Feb 2019 a workshop took place with a focus on PANDA related physics and technology at ICTP in Sao Paolo/Brazil bringing South American researcher in close contact with PANDA science and construction. The meeting was well attended (about 60 registrants) and included also a panel discussion about the strategic development of this field in Brazil for an eventual membership in PANDA and the discussion about joint funding opportunities.

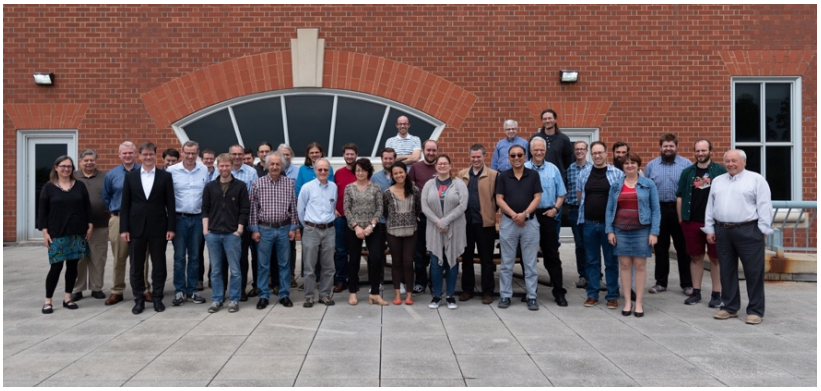

A GlueX-PANDA Workshop has taken place at George Washington University/USA in May 2019. It was a vibrant meeting on many aspects of potential cooperation. In the very constructive atmosphere, we identified several common areas of interest and potential cooperation, which include DIRC and PID, EMC, Machine Learning, Analysis framework and Education.

During the recent BESIII Collaboration Meeting at IHEP/Beijing/China in Nov 2019, PANDA has had the opportunity to present itself with two packed sessions.

A topic which was started and will be a major focus of the collaboration will be all aspects of Outreach, including social media, press and the face-2-face education in masterclasses as soon as this is achievable given the current world-wide virus situation. This goes hand in hand with Diversity aspects and measures which we will investigate and implement.

Given the virus situation the outlook for 2020 is not simple, but everything will be done to keep up with the original schedule as good as possible.

PANDA Management Team in 2019

Spokesperson ..... Klaus Peters/GSI & U Frankfurt/Germany

Deputy Spokesperson ..... Tord Johansson/U Uppsala/Sweden

Collaboration Board Chair ..... Kai-Thomas Brinkmann/U Giessen/Germany (until 06/2019)

..... Frank Goldenbaum/FZ Jülich/Germany (since 07/2019)

Deputy Collaboration Board Chair ..... Andrey Ryazantsev/IHEP Protvino/Russia

Technical Coordinator ..... Lars Schmitt/FAIR

Deputy Technical Coordinator ..... Anastasios Belias/GSI/Germany

Finance Coordinator ..... Ralph Böhm/FAIR

Physics Coordinator ..... Johan Messchendorp/KVI-CART Groningen/The Netherlands

Deputy Physics Coordinator ..... Karin Schönning/U Uppsala/Sweden

Computing Coordinator ..... Tobias Stockmanns/FZ Jülich/Germany

Deputy Computing Coordinator ..... Ralf Kliemt/HI Mainz/Germany

Contact Person ..... Frank Maas/HI Mainz/Germany (until 11/2019)

complemented by Diego Bettoni, LNL/Italy, Alexander Vasiliev/IHEP Protvino/Russia, and Ulrich Wiedner/U Bochum/Germany as additional members from the PANDA Strategy Board,

Alaa Dbeyssi/Hi Mainz/Germany, Fritz-Herbert Heinsius/Uni Bochum/Germany), and Alfons Khoukaz/Uni Münster/Germany as chairs of the Speakers Committee, the Membership Committee of PANDA, and the Governance Rule Writing Group respectively. In addition, Miriam Fritsch/Uni Bochum/Germany represented the non-pbar physics working group.

The whole is more than the sum of its parts. This is sometimes said and for the proton, this expression is literally true. The sum of the masses of its valence quarks accounts for less than 2% of the proton's total mass, with the rest resulting from the kinetic and binding energies among quarks due to dynamics of the strong interaction. Quantum Chromodynamics (QCD) is the accepted theory of the strong interaction and describes the properties of quarks and their interactions through gluons, the force mediator of the strong interaction. Despite the success of QCD in predicting processes at high energies, at low energies, the theory becomes strongly coupled as α_s becomes large. In this non-perturbative regime, it is still hard to make predictions from first principles.

The complexity of the strongly coupled many-body system in non-perturbative QCD gives rise to many questions: What are the effective degrees of freedom which systematically describe resonances and bound states? Where are the exotic resonances and bound states predicted by QCD? How do bound quark systems interact? What is the residual structure of the hadronic systems? Thus, the central goal of the PANDA experiment is the elementary understanding of hadrons using the power of an antiproton beam on hydrogen or nuclear targets. This very process, the annihilation of nucleons, creates a rich variety of hadrons with respect to other experimental probes with the additional advantage of a well-defined and flavor-blind initial state. High precision mass scanning complements this and underlines the uniqueness of the project. All this has been proven in the past to be a universal tool for carrying out the necessary investigations and in order to utilize antiprotons for hadron physics the PANDA (anti**P**roton **AN**nihilation in **DA**rmstadt) collaboration has been formed and is today a cooperation of almost 500 scientists from 20 countries.

The experiment will be located at the Facility for Antiproton and Ion Research (FAIR), an accelerator facility leading the European research in nuclear and hadron physics in the coming decade. It builds on the experience and technological developments from the existing GSI facility, and incorporates new technological concepts, such as rapidly cycling super-conducting magnets. It will e.g. address a wide range of physics topics in the fields of nuclear structure, nuclear matter, atomic and plasma physics.

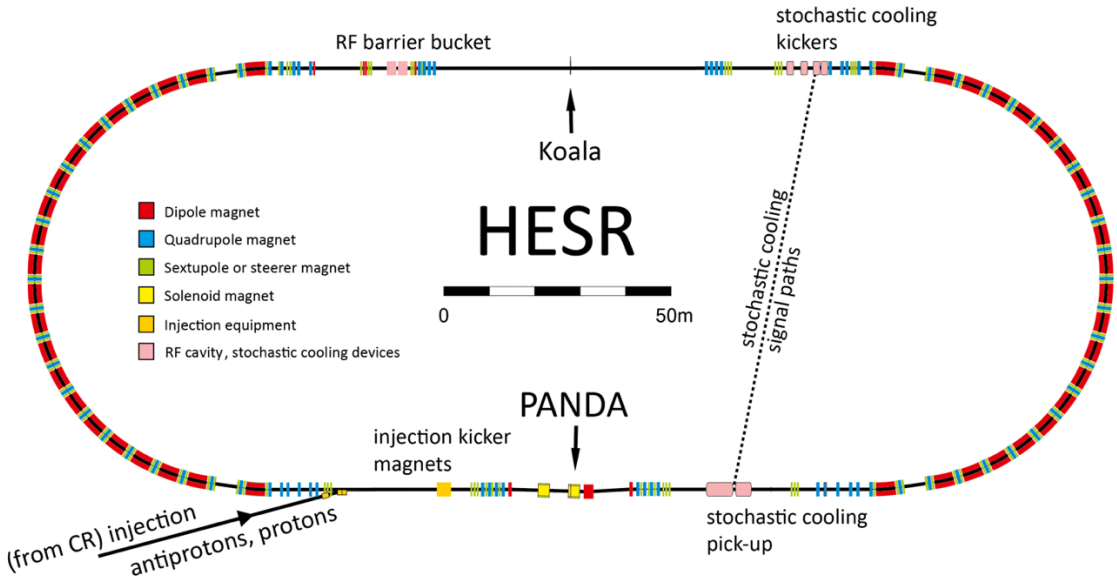

Figure 1: High Energy Storage Ring at FAIR. The PANDA detector is located in one of the straight sections where the antiproton beam interacts with a fixed target. Koala is a precision scattering experiment for systematic luminosity studies.

An important feature of the new antiproton facility is the combination of dense internal targets and phase-space cooled beams in the High Energy Storage Ring (HESR) which hosts PANDA as an in-beam experiment. It will allow two operation modes: A high-resolution mode with a momentum spread down to a few times 10^{-5} and beam intensities up to 10^{10} using a powerful stochastic cooling system, and a high-luminosity mode with beam intensities up to 10^{11} in a later stage. The HESR is filled by the Collector Ring (CR) which accumulates by stacking the antiprotons every 10 seconds from the collision of 2.5×10^{13} protons of 29 GeV in a 50 ns bunch on the production target.

The HESR lattice is designed as a racetrack shaped ring, consisting of two 180° arc sections connected by two long straight sections. One straight section will host the installation of the PANDA experiment with an internal target as well as RF cavities, injection kickers, and septa (see Fig. 1). The other section will mainly be occupied by an electron cooler at a later stage and will host smaller experiments for nuclear and atomic physics with ion beams. For stochastic cooling, pickup and kicker tanks are located in the straight sections, opposite to each other. The momentum of the antiprotons ranges from 1.5 to 15 GeV/*c*, allowing for a wide variety of physics channels (see Fig. 2).

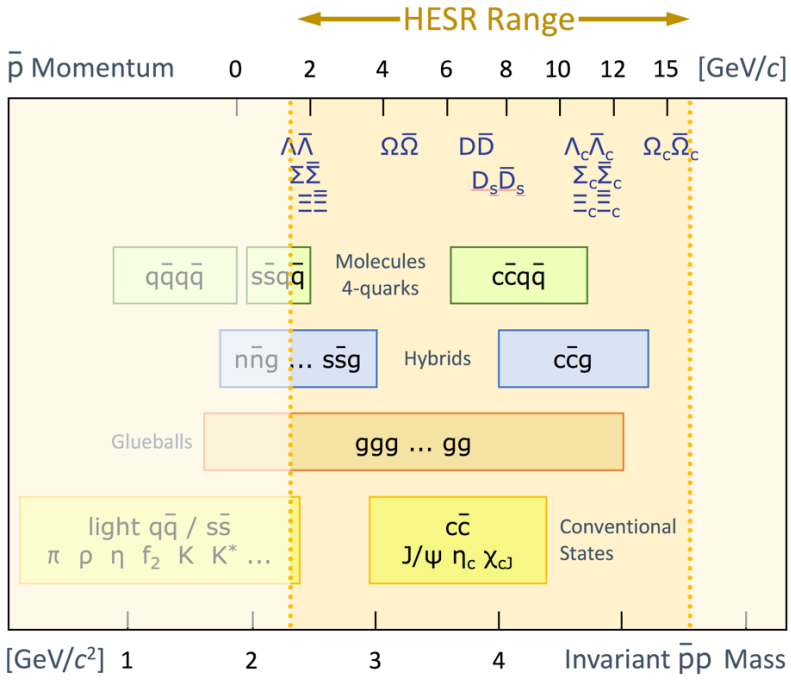

Figure 2: Some of the many accessible hadron species with PANDA and HESR.

The PANDA experiment belongs to a new generation of hadron physics experiments, hereby building on the experiences and successes of previous generations. It features a modern multipurpose detector (see Fig. 3). The combination of a high-quality antiproton beam at the HESR, an unprecedented annihilation rate, and a sophisticated event filtering, is an ideal experimental infrastructure to address important questions to all aspects of this field by collecting large statistics and high-quality exclusive data to test QCD in the non-perturbative regime. In the following, we will outline a few of the physics aspects that will be addressed using this facility (see Ref [1,2] for more details).

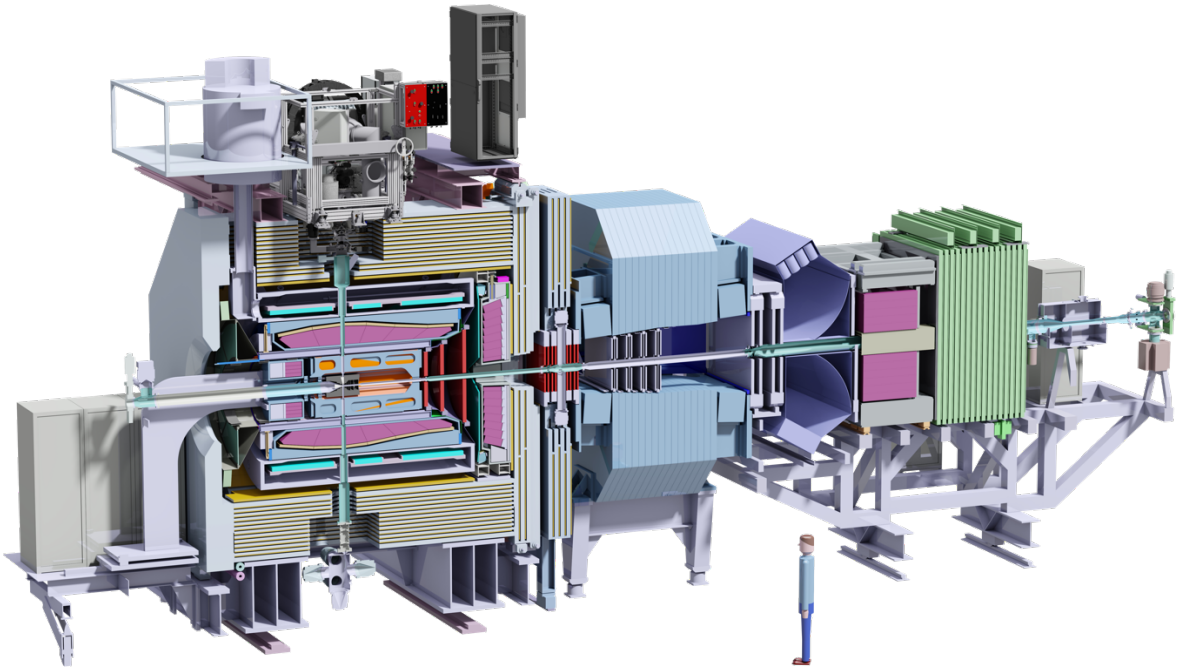

Figure 3: CAD drawing of the full PANDA Detector. The Day-1 configuration (described later) is currently under construction and will be completed and commissioned in 2024.

PANDA will copiously produce anti-hyperon-hyperon pairs through the reaction $\bar{p}p \rightarrow Y\bar{Y}$. The energy scale is given by the mass of the strange quark (m_s~100 MeV/c^2), which is below, but near the strong coupling scale Λ_{QCD}. This corresponds to the confinement domain, where our knowledge of the strong interaction is scarce. Therefore, the relevant degrees of freedom – quarks and gluons or hadrons – remain unclear. Spin observables have been proven to be very sensitive to the underlying degrees of freedom of the model describing the interaction. The high cross section for hyperon pair production using antiproton interactions will provide the necessary high statistics to access spin observables with sufficient precision. In addition, so far unmeasured multi-strange hyperons are accessible with PANDA. In particular, seven polarization parameters of the spin 3/2 Ω-hyperon can be extracted for the first time.

This large production cross section will also enable several innovative studies of systems containing two or even more units of (anti-)strangeness in antiproton-nucleus collisions at the PANDA experiment. The interaction of antibaryons in nuclei provides a unique opportunity to elucidate strong in-medium effects in baryonic systems. Quantitative information on the anti-hyperon potentials will be obtained for the first time via exclusive anti-hyperon-hyperon pair production close to its production threshold in antiproton-nucleus interactions. After pioneering studies of the Λ potential during the first phase of PANDA, the Ξ and even the Ω potential can be explored once the full luminosity is available. Baryons with strangeness embedded in the nuclear environment, hypernuclei or hyper-atoms, are the only available tool to approach the many-body aspect of the three-flavor strong interaction. A new key measurement will be high resolution γ-spectroscopy of excited states in several doubly strange ΛΛ-hypernuclei. Hypernuclear studies would result also in valuable insights to astrophysics as well, such as the Hyperon-puzzle of neutron stars and mechanisms of core-collapse supernovae.

The field of charmonium spectroscopy is an exciting field with many discoveries in the past 15 years. Many predicted states have not been observed and, on the other hand, masses, widths, and decay rates of many unexpected states (XYZ states) have been measured. Until today, a coherent picture cannot be drawn from what is available experimentally. PANDA will contribute to this field in two unique ways: a) in explorative studies in many-body experiments to search

for high-spin and spin-exotic states and b) by a precision measurement of the mass and width (or more generally the line-shapes) of any neutral charmonium-like state. The very small momentum spread of the antiproton beam allows a determination of the width, for example of the X(3872), with an accuracy of 50 keV. Such an accuracy will provide a decisive measurement on the nature of the narrow X(3872). This technique can also be used to investigate excitation curves of open-charm final states, like e.g. $D_sD_{s0}^*(2317)$ to measure the width of the respective $D_{s0}^*(2317)$.

Furthermore, antiproton annihilations allow for the study of a rich variety of nucleon structure observables in large (partly) unexplored areas such as the kinematical regime that corresponds to the time-like (positive, s-channel) momentum transfer of the virtual photon. The electromagnetic form factors of the proton, Transition Distribution Amplitudes (TDA), Wide Angle Compton Scattering (WACS), and Drell-Yan processes for accessing Transition Momentum-Dependent Parton-Distribution Functions (TMD-PDF) are examples of those variables. Fig. 4 shows how crossing symmetry e.g. connects space- and time-like regions.

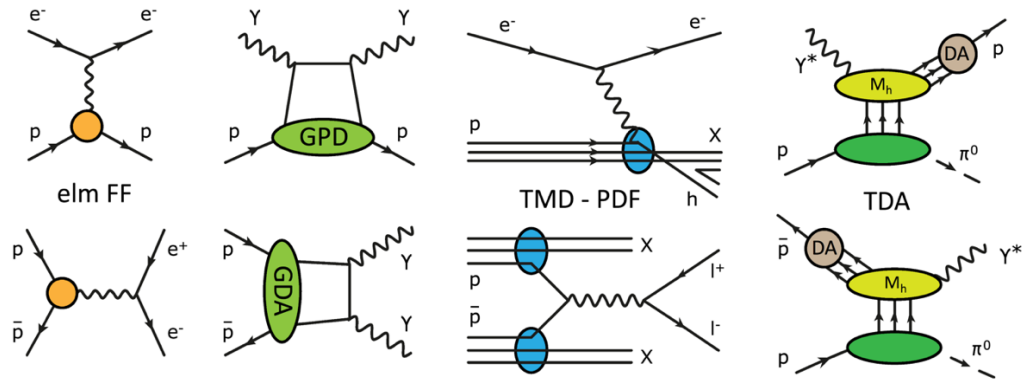

Figure 4: Crossed channel diagrams that relate electromagnetic scattering off the proton to lepton/photon pair production from antiproton-proton annihilations (elm FF=electromagnetic form-factor, GPD=Generalized Parton Distribution, GDA=Generalized Distribution Amplitudes, M_h=hard process amplitude, DA=Distribution Amplitude, see Ref [1,3] for more details).

Experiments accessing the region of positive momentum transfer squared complement the studies of the nucleon structure from the lepton scattering experiments (negative q^2). They provide experimental support to the non-perturbative approaches used to describe the high energy electromagnetic processes in different regimes. Fig. 4 shows crossed channel diagrams that allow to extract the same functions, like for the case of TDAs and TMD PDFs, or to extend their measurements like for the case of form factors and GDAs, in/to different kinematical regimes (space- and time-like regions).

The main objectives of the design of the PANDA experiment are to achieve almost 4π acceptance, high resolution for tracking, particle identification and calorimetry, high-rate capabilities and a versatile readout and event selection. To obtain a good momentum resolution, the detector will be composed of two magnetic spectrometers: The Target Spectrometer (TS), based on a superconducting solenoid magnet surrounding the interaction point, for particle tracks at large angles and the Forward Spectrometer (FS), based on a dipole magnet, for small angle tracks. In both spectrometer parts, tracking, charged-particle identification, electromagnetic calorimetry and muon identification will be available to allow to detect the complete spectrum of final states relevant for the PANDA physics objectives.

The TS has a typical onion-like structure, very much like the detectors used for the B-Factories Babar and Belle: A cluster jet or pellet target system will be used to provide either a cluster beam of a target gas or frozen hydrogen pellets. Thin foils or noble gasses will be used for antiproton-nucleus studies. The interaction point is surrounded by the Micro Vertex Detector

(MVD) which has a vertex resolution of about 50 µm in transverse and 100 µm along the beam direction. Surrounding the MVD, the Straw Tube Tracker and Gas Electron Multiplier (GEM) stations will be used for tracking charged particles ($\Delta p_T/p_T$ = 1.2%) in the magnetic field. Photons and the energy of electrons will be reconstructed with the Electromagnetic Calorimeter (EMC). The EMC consists of a barrel (azimuthal angle 22° to 140°), a forward endcap (down to the opening for the FS) and backward endcap (145° to 170°) and consists of about 16,000 $PbWO_4$ crystals providing an energy resolution of 1.5%/√E, whereby E is given in units of GeV. Particle identification of pions, kaons and protons will utilize information from a Time-of-Flight system (ToF), a cylindrical DIRC (Detection of Internally Reflected Cherenkov light), and a forward Disc DIRC detector. The ToF will use scintillating tiles with Silicon Photomultiplier readout. The cylindrical DIRC is a bar-type DIRC with quartz-prisms, while the Disc DIRC uses large quartz plates. The solenoid magnet will provide a homogeneous magnetic field up to 2 T in the beam direction. The segmented yoke is instrumented with chambers for muon identification.

The FS covers polar angles below 10° horizontally and 5° vertically. Charged particles will be detected using the Forward Tracking System, which consists of multiple straw tube layers, in conjunction with a dipole magnet with variable field depending on the incident antiproton momentum. The momentum resolution for tracks above 1 GeV/c is better than 1%. A Forward Time-of-Flight and an aerogel-based Ring Imaging Cherenkov Counter detector will provide particle identification. A Shashlyk-type Calorimeter with an energy resolution of 3%/√E is followed by the Muon Range System for muon detection. At the forward end, the Luminosity Detector uses elastic scattering of antiprotons on protons to determine the interaction rate measuring antiprotons deflected at low angles. A detailed description of the PANDA detector and its components can be found at [4].

As the detector response of background events is very similar to that of the decay of the exotic states, the use of a conventional triggered readout scheme, where a limited number of subdetectors generates a trigger signal that engages the readout of the complete detector, is not practical. Therefore, a new type of intelligent readout is being developed, where kinematical constraints are imposed online on reconstructed events. This technique is dubbed as “triggerless readout” and allows adjusting the data selection to numerous physics channels. A data reduction factor of up to ~10^3 is expected to be achieved by employing this technique for the whole detector, resulting in a data rate of ~10^4 events/s (or, equivalently, 200 MB/s) that will then be sent to storage for offline processing and analysis.

References and further reading

[1] M.F.M. Lutz et al., *Physics Performance Report for PANDA: Strong Interaction Studies with Antiprotons*, arXiv:0903.3905 (2009)

[2] M.F.M. Lutz et al., *Resonances in QCD*, Nucl.Phys. A948 (2016) 93, https://doi.org/10.1016/j.nuclphysa.2016.01.070

[3] R.A. Briceno et al., *Issues and Opportunities in Exotic Hadrons,* Chin.Phys. C40 (2016) no.4, 042001, see also INT-PUB-15-066, JLAB-THY-15-2174, FERMILAB-PUB-15-652-T

[4] U. Wiedner, *Future Prospects for Hadron Physics at PANDA*, Prog.Part.Nucl.Phys. 66 (2011) 477-518, 10.1016/j.ppnp.2011.04.001

[5] https://panda.gsi.de

Already in the first two phases of PANDA several different scientific topics within subatomic physics will be addressed. These two, referred to as *Phase-1* and *Phase-2*, both occur during the period without the RESR that comes with *Phase-3*. In the transition from Phase-1 to Phase-2 additional detector components will be installed to have the full setup of PANDA available, mainly for a better coverage for particle identification. Phase-3 corresponds to the full design luminosity, which is possible with the additional storage ring available beyond MSV0-3 ($\int L > 10$ fb^{-1}). Thus for our considerations, the luminosity will be limited in Phase-1 and Phase-2 to $L = 2 \cdot 10^{31}$ cm^{-2}s^{-1}. During Phase-1 and -2, we aim to collect data corresponding to an integrated luminosity of about $\int L = 0.5$ fb^{-1} each, using the so-called *Start-setup* of PANDA described below. The period leading up to the very first antiproton runs of PANDA is referred to as *Day-1*. During this period, we will perform the first necessary steps towards the realization of Phase-1 and -2. In the text we quote how much of the program can be accomplished in these phases with the sum Phase-1 plus -2 defined as 100%. We have used the amount of required data to quantify the fraction of accomplishment.

Below, we briefly discuss the present goals of the physics pillars for the first two phases (including comments on the respective competition), followed by a discussion of the activities at Day-1 with quantitative statements. However, we are prepared that new discoveries may alter these plans.

Hadron spectroscopy

The first pillar is devoted to provide precision data for hadron spectroscopy with light to charm constituent quarks, and gluons. Concerning the light-quark and gluon sector, we plan to map out the glueball spectrum and to search for exotic forms of hybrids and meson-like or molecular states.

Final states best suited for that include one or multiple ϕ, ω, η, J/ψ as well as D and D_s mesons since their production is OZI suppressed due to the large flavor component, and thus those channels have reduced conventional matter content.

The data we foresee to harvest are complementary to studies conducted at BESIII, COMPASS, GlueX, and Clas12 due to various reasons like the probe, the analysis technique and the accessible quantum numbers. The LEAR facility has demonstrated the strong advantage of using antiprotons for gluon-rich matter such as various scalar states that were first discovered using antiproton annihilations including the candidate for the glueball ground state, *i.e.* the $f_0(1500)$. PANDA will extend these measurements by probing a sufficiently larger energy range (E_{cms} = 2-5.5 GeV) and with a detector capable to perform a fully exclusive study of practically all final states. As demonstrated by LEAR, the cross sections are spectacularly high in contrast to reactions with electromagnetic probes. Already with lower luminosities, this gives excellent prospects for the search for massive glueballs with $J^{PC} = 2^{++}$ and 0^{-+}, hybrid states with gluonic degrees of freedom and exotic quantum numbers as well as meson-like states with light and strange quarks. The analysis technique at PANDA is based on PWA of exclusive final states and constraints on the initial state for the ease of reliable quantum number assignments that are crucial for the interpretation of the data. This is superior to scattering experiment in terms of systematics and backgrounds and can systematically be extended to the hidden and open-charm sector. This will *e.g.* shed new light on the recently discovered charmonium-like *XYZ*-spectrum with precision line-shape scans (with a resolution of about 50 keV/c^2 per point). In particular, it will allow for searches in the high spin segment (up to J = 6) or at larger mass (up to 5.5 GeV/c^2) to complement the existing findings such as $X(3872)$, $Z_c(3900)$ and $Z_c(4020)$ (to name a few) for which most of the decay channels are not found yet and counter parts for an

understanding of the spectrum are missing. In Phase-1, we expect to complete 75% and 25% of our light-(include strange-)quark-exotics and charm-exotics programs, respectively.

Hyperon physics

The second physics pillar of PANDA is the pairwise production of mesons and baryons with open-strangeness and charmness in $\bar{p}p$ annihilations. This is truly unique in the world and will provide insight in the underlying mechanisms that play a role in the creation of strange and charm quark pairs. For the Phase-1 and Phase-2 programs of PANDA, we foresee to exploit the pair production of |S|=1, 2, and 3 and |C|=1 baryons and mesons near their production thresholds. It delivers a rigorous test for the validity of few-body models at various mass and energy scales. The self-analyzing feature of weakly-decaying hyperons gives experimental access to spin observables such as polarization and spin correlations, which are sensitive to the production mechanism. A multidimensional analysis of the particle-antiparticle symmetric final state provides a model-independent test of CP violation in baryon decays. This has to be seen in the context of the long-standing puzzle of the matter-antimatter asymmetry of the Universe.

We expect to complete in Phase-1 100%, 90%, 10%, and 10% of the hyperon spin program for |S|=1, 2, 3, and |C|=1, respectively on the basis of 7M , 4M, 90k, and 100 reconstructed events per day for $\bar{p}p \to \Lambda\overline{\Lambda}, \Lambda\overline{\Sigma}, \Xi\overline{\Xi}, \Omega\overline{\Omega}$ near threshold in Phase-1 respectively.

The associated production also will provide the opportunity to extensively investigate the spectrum of the charm and strange sector. This allows for a tagging method, an ideal tool for spectroscopy purposes near production thresholds where the missing-mass resolution is optimal and the background is small. Limitations in the luminosity are compensated by the huge cross sections (up to microbarns) that can be expected because of past experience, in particular for |S|=1, 2 hyperons. In general, the production cross sections of |S|=2 states with antiprotons are two- or three-orders in magnitude larger than that of photons. PANDA will be able to study the |S|=3 sector, where only very few experiments can contribute measurements. Furthermore, the antiproton probe makes PANDA sensitive to states that do not couple to photons or kaons. We expect to complete in Phase-1 70%, 40%, but 0% of our programs for |S|=2, 3, and |C|=1, respectively.

Proton structure

Proton structure experiments with electromagnetic final-states in antiproton-proton collisions are the third physics pillar of PANDA. In the first phases of PANDA, we want to measure the electric and magnetic form factors, $|G_E|$ and $|G_M|$, and their ratios at various q^2 values in $\bar{p}p \to l^+l^-$. These time-like electromagnetic form-factor studies are a necessary complement to the space-like counterpart in lepton-scattering experiments. The foreseen PANDA measurements will extend the time-like data of electron-positron annihilation experiments, such as the ones conducted at BESIII, substantially in terms of energy range as well as accuracy. PANDA will collect data that are sensitive to probe the unphysical regime, $4m_e^2 < q^2 < 4m_p^2$ by exploiting a final-state with an additional pion that brings the (anti)proton offshell. The present-day accuracy will be improved from 20% at low q^2 values to 3%. Combining data from BESIII (yet unpublished) and PANDA, the analytical nature of the form factors can be studied. Besides these unique measurements, PANDA will be the first experiment capable to measure the proton time-like form factors in both e^+e^- and $\mu^+\mu^-$ final states. It might offer new insights in the proton radius puzzle by testing the lepton universality in these reactions.

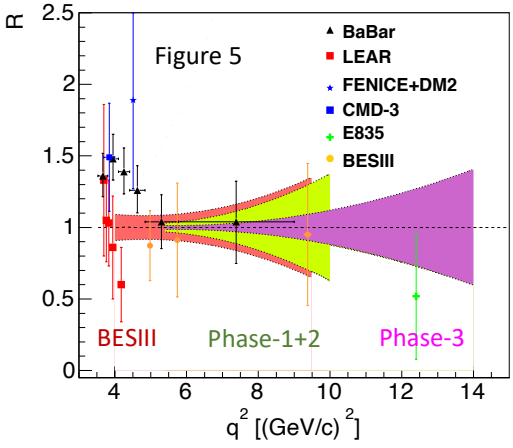

Recent Monte Carlo (MC) studies have been performed for the Phase-1 setup as well as for the full setup at Phase-3. They have demonstrated that the PANDA start setup has the capability of successfully suppressing the huge background from the di-pion channel provided that satisfactory knowledge is obtained on the background dynamics. PANDA can provide data for detailed studies of multi-pion production in antiproton-proton annihilations. These data will serve as input to QCD calculations. Fig. 5 shows a comparison of existing data on $R = |G_E|/|G_M|$, the size of the errors of the so-far unpublished BESIII measurement (red-shaded area for comparison) and the error forecast for PANDA Phase-1+Phase-2 (green-shaded area). 50% of this program will be completed during Phase-1. The pink-shaded area indicates the error that we will achieve at Phase-3 with a factor of ten higher beam intensity.

Strange hadrons in nuclei

The fourth pillar of the Phase-1/2 program is dedicated to study the properties of hadrons in a nuclear medium. Firstly, we propose studies of the antihyperon-nucleus potential, accessible via the associated production of hyperon pairs close to the production threshold, which cannot be studied at any other laboratory in the world. It offers essential information for the interpretation of data from heavy-ion collision experiments. Furthermore, the foreseen program includes measurements of the basic (mass, width) parameters of hidden-charm states at nuclear densities. This might give complementary information that helps to shed light on the formation of hadrons and measures signatures that could point to the (partial) restoration of chiral symmetry. Also, in the context of color transparency we can deliver significant contributions that exceed those of other experiments, *e.g.* access to other final states due to the $\bar{p}N$ entrance channel. We expect to complete 70% of this program in Phase-1.

Furthermore, antiprotons can be used to implant hyperon pairs into a nucleus as a Phase-2 program. PANDA offers also the unique possibility to search for X-ray transitions from very heavy hyperatoms as e.g. Ξ^{-208}Pb which is not possible at other labs. This will complement experiments at J-PARC which attempt to measure X-rays in medium-heavy nuclei. The measurement at PANDA will for the first time allow to constrain the interaction of Ξ^--hyperons in the neutron skin. In a later stage, PANDA will extend the studies on double hypernuclei by performing for the first-time high resolution γ-spectroscopy of these nuclei. Thus, PANDA complements measurements of ground state masses of double hypernuclei in emulsions at J-PARC by the E07 Collaboration or the production of excited resonant states in heavy ion reactions which may for example be performed in future by the CBM Collaboration. Both studies are unique and cannot be done elsewhere. In Phase-3 we are planning to study charm in nuclei as well.

Early Science

Under the assumption that the starting luminosity at Day-1 could be significantly below design, the goal is to primarily concentrate on channels with large cross sections (μb) and relatively simple event topologies. Also, the setup will be reduced due to fabrication schedules and available funds. We expect to collect in the order of 5 pb^{-1} of data, which will be roughly 1% of the total Phase-1 integrated luminosity. Thus, one has to differentiate between two aspects. There is the Day-1 setup, which seamlessly evolves to the Phase-1 setup as more components get ready, and the initial Day-1 luminosity, which is expected to increase quickly to the desired Phase-1/2 beam intensity to eventually allow for the full MSV0-3 program. Given these preconditions of Day-1, we have identified i) flagship experiments with a guaranteed physics outcome, ii) feasibility studies with a high discovery potential, and iii) development activities to realize the full physics program. These three categories of experiments will provide data for all pillars of PANDA. The focus will, to a large extent, be on studying the various production mechanisms of strange and partly charm-rich hadrons. In addition, we will map out the elastic

$\bar{p}p$ cross section for the ease of luminosity calibration. Below, we briefly illustrate a few typical cases of each of the three categories as indicators of the Day-1 capabilities of PANDA.

Flagship studies

As a typical flagship study for Day-1 within the light-meson and gluonic matter spectroscopy program of PANDA, we consider relatively simple two-body final-state reactions that are easily identifiable and, preferably, are flavor-blind in order to be sensitive to gluon-rich matter (like massive glueballs). A key example is $\bar{p}p \to \phi\phi$ which has been first observed by Jetset in the late 1990's and which has a huge cross section in the order of a few µb at threshold, about 100 times larger than expected from the OZI rule. This has been interpreted as an indication of a strong tensor glueball contribution. We would be able to study this reaction at energies beyond what has been achieved at LEAR and being extendable with additional mesons, *e.g.* π^0. This would also be an excellent case to benchmark the partial-wave analysis tools[1].

We expect to achieve a significant physics output by studying the production of antihyperon-hyperon pairs for both |S|=1 (i.e. $\bar{p}p \to \bar{\Lambda}\Lambda$) and |S|=2 (i.e. $\bar{p}p \to \bar{\Xi}\Xi$) systems near their corresponding production thresholds at ~1.64 GeV/*c* and ~4 GeV/*c*, respectively. Differential cross sections and polarization observables can be measured within a few days, whereby the systematic uncertainty will be the limiting factor. The study of the $\bar{p}p \to \bar{\Lambda}\Lambda$ channel at 1.64 GeV/*c* will be benchmarked using published data from LEAR as a reference. At 4 GeV/*c*, both |S|=1 and |S|=2 systems will be unique and new measurements.

The hyperon-antihyperon production studies at threshold energies can be extended using nuclear targets. We then would have access to the relative asymmetry between the transverse and longitudinal momentum of the two hyperons. These observables are of particular interest since they are sensitive to the antihyperon-nucleus potential. Their measurements can be conducted with sufficient data samples in only one week of data collection at a luminosity of about 10^{30} cm^{-2}s^{-1} and would not only be exclusive in the world, but also very valuable for the heavy-ion physics community.

Feasibility studies with discovery potential

The cross sections in the µb range (Fig. 6) and the promising perspective of associated hyperon production provides a basis for baryon spectroscopy measurements with strangeness degrees-of-freedom. Even with a limited setup at Day-1, excited baryons with strangeness contents can be studied using the missing-mass technique as a first step. In particular, the excited spectrum of |S|=2 baryons (Ξ) give information, *e.g.* mass and partial width, and are complementary to the baryon spectroscopy studies conducted at JLab.

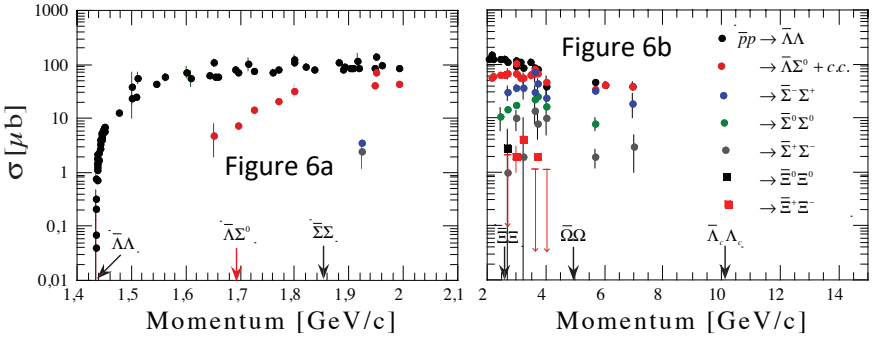

The hidden-charm sector above the open-charm threshold is one of the mysteries since many unconventional charmonium states have been discovered in the past decades. For the Day-1 program, it is intriguing to open up a new territory with the use of $\bar{p}p$ or $\bar{p}n$ reactions to search for yet unobserved charged Z-states. Such discoveries would be complementary to the spectrum of recently discovered $J^P = 1^+$ Z-states in e^+e^- collision experiments (BESIII, CLEO-c, BELLE2). The $\bar{p}n$ reaction can be used to produce these charged states without a recoil particle. These states are easily identifiable via their decay into a J/ψ. The final state will therefore be composed of a few charged pions and a lepton pair from the J/ψ, for which the Day-1 setup will

have sufficient efficiency and acceptance. With the available energy at PANDA, we can study heavier Z-states than BESIII and/or states with a spin that exceeds $J^P = 1^+$.

Development of novel techniques

One of the features of PANDA is the usage of stochastically cooled antiprotons with an excellent momentum resolution. Such a beam allows to perform an energy/mass scan of various narrow states with hidden-charm and a variety of spin and parity. One of the Phase-1 goals is a scan of the mysterious X(3872). The measurement of the width, or the line shape in general, of this very narrow resonance could conclude its nature. However, the prospects of this study at Day-1 are not very promising since the production cross section is less than 50 nb. Instead, we will develop and validate the line-scan method by applying it on one of the well-known conventional charmonium states below the open-charm threshold. The vector charmonium states would be the best candidates because of their relatively large coupling to $\bar{p}p$.

The electromagnetic form factor studies require good knowledge on the multi-pion background channels. We plan to measure extensively differential cross sections of these channels that will be used as input to QCD models in order to develop accurate event generators. Since the cross sections of these background channels are large and the event topology fairly simple, it will be ideally suited as a Day-1 development study. The goal would be to validate the simulation result with experimental data that the background can be suppressed sufficiently enough to be able to identify $\bar{p}p \to \mu^+\mu^-/(\pi^0)e^+e^-$.

PANDA Straw Tube Systems @ HADES

A major aspect of the HADES and PANDA physics program is the investigation of the static properties and decay modes of excited hyperons. Due to the high boost needed to produce these systems at HADES, the reconstruction of forward-emitted protons up to polar angles of 7° is particularly important to reconstruct protons from hyperon decay. Since detector modules of the PANDA Forward Tracker stations FTRK3/4 and FTRK5/6 ideally match this acceptance hole in HADES, a FAIR Phase-0 project is ongoing to employ these PANDA detectors as the HADES forward Straw Tracking Stations STS1 and STS2, respectively. The PANDA tracking stations are part of an ongoing major upgrade of HADES, which includes not only expanded acceptance to track forward-emitted charged particles but also an RPC system for Time of Flight measurements, a large acceptance EM calorimeter, improved photo-efficiency of the RICH detector and a major rate increase of the DAQ system.

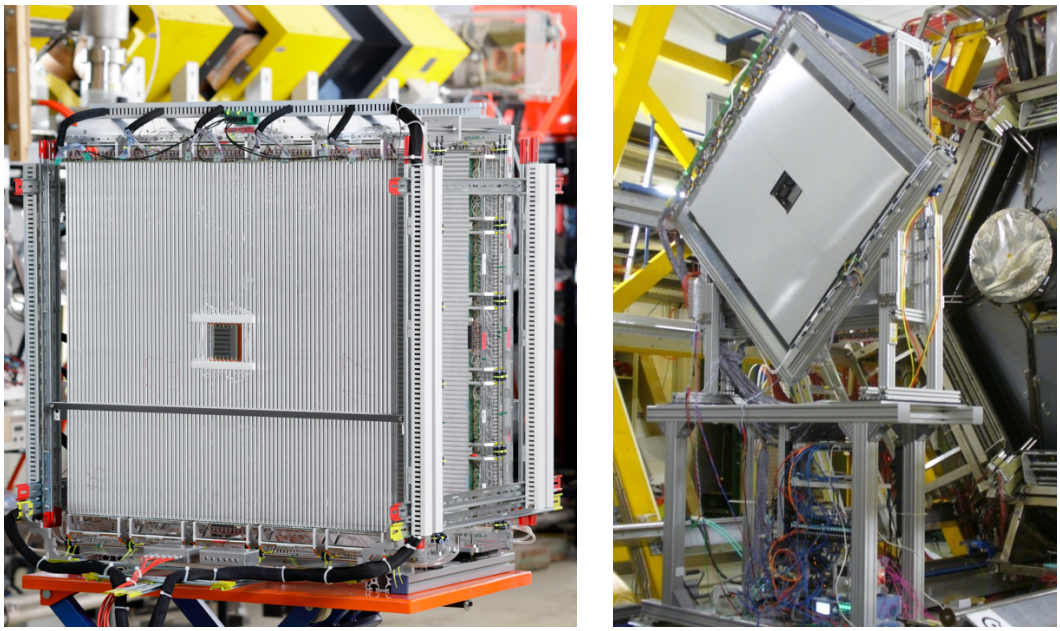

Figure 7: Tracking stations STS1 (left) and STS2 (right). The STS1 is ready for transport to GSI and the STS2 is already installed at HADES, which is partially visible in the background.

STS1

The STS1 station was produced in Jülich and consists of 704 straws arranged into a stack of four double-layers, each consisting of four modules with 32 straws of 76.6 cm length and one center module with 48 straws. Each center module features an 8 cm x 8 cm hole for the beam. The first and last double-layer are orientated vertically and both intermediate double-layers are arranged horizontally. For setting up and pre-testing the STS1, the data-acquisition system was installed and updated. The same DAQ system will be also used for the PANDA-STT system. After finishing the functional system tests, the STS1 will be installed in the HADES spectrometer at GSI in spring 2020 to be commissioned by a test beamtime of the upgraded HADES spectrometer, which is scheduled to take place in early June 2020.

STS2

The tracking station STS2 was built at the Jagiellonian University in Krakow and has recently been installed in HADES. The STS2 consists of a total of 1024 straws that are arranged into four

identical double-layers. The first two double-layers are inclined by 90° and 0° with respect to vertical, and the next double-layers are inclined by +45° and -45° for unambiguous reconstruction of multi-track events. Each double-layer consists of 8 modules with 32 straws each. Six modules have a length of 125 cm, and the two central ones are 52.5 cm each, to create an opening for the beam. Each double-layer has an individual high voltage and the straws are supplied with Ar+CO_2 (90:10) gas mixture at 2 bar absolute pressure using a dedicated gas system built in the Institute of Nuclear Physics PAN in Krakow in collaboration with the Research Center Jülich. The high voltage system and the gas system are controlled using the EPICS environment and a graphical user interface developed in the Control System Studio framework. The readout consists of 16 channel front-end electronics cards, each containing two PASTTREC chips. The drift time and the time-over-threshold of the straw tube pulses are measured with the Trigger Readout Boards version 3. The readout of the tracking stations has been integrated with the HADES DAQ system.

Simulated physics performance

The electromagnetic (EM) decay of excited hyperons states is a very sensitive probe of the structure of hyperons, since it provides a relatively clean probe of the wave functions of the initial and final baryon states. The influence of the STS in the HADES Forward Detector has been evaluated for several benchmark channels: Ξ^- and ΛΛ production, Λ(1520), Λ(1405) and Σ(1385) hyperon resonances production and their electromagnetic decays via real and virtual (i.e. Dalitz decays) photons.

Simulation results show that the Forward Detector provides a significant increase in the amount of statistics (e.g. a factor 9 for Ξ^-, about a factor 2.5 for hyperon resonances and ΛΛ events can only be reconstructed including the Forward Detector) and acceptance (nearly full polar angle). The expected count rates are limited by the HADES DAQ and detailed estimates have been made under the following expected conditions: A proton beam with T=4.5 GeV, a flux of 10^8 p/s, the HADES liquid hydrogen target, 50 % DAQ duty cycle and a four-week measurement. Under these conditions, which correspond to an instantaneous luminosity of 2 x 10^{31} /(cm^2s), about 600-700 events are estimated for virtual photon decays of hyperon resonances. An increase of the count rates by a factor 7 is expected for a Polyethylene target. For the real photon decay of Σ(1385), Λ(1405), and Λ(1520) hyperons the photons are measured in the EMC. The largest source of background is expected from the non-resonant $pK^+\Lambda\pi^0$ final state, in which one photon from the π^0 decay is not detected. Under the above-mentioned conditions, a total of around 200 counts/day are expected for the sum of these three states.

PANDA@MAMI

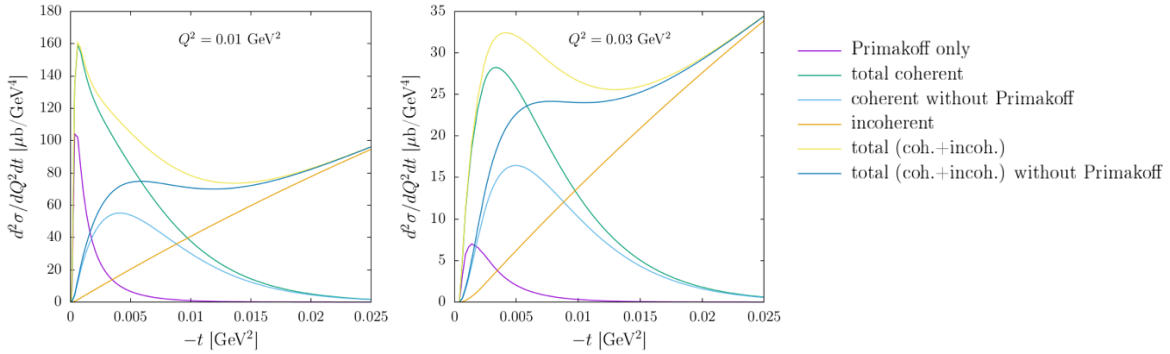

Figure 8: Differential cross section for the π^0 electroproduction on a ^{181}Ta nucleus at a beam energy of 1.5 GeV and electron scattering angle between 5° and 15°. The cross section is shown as a function of the momentum transfer to the target t for two different values of the momentum transfer from the electron Q^2.

As FAIR Phase-0 project at MAMI, the measurement of the π^0 transition form factor (TFF) through the coherent electroproduction of neutral pions on nuclei has been proposed. The TFF enters the cross section via the Primakoff contribution, which can be isolated at small momentum transfer *t* to the target. Until recently, the cross section had been estimated, using the Primakoff contribution only, neglecting the hadronic production, which gives the largest contribution to the total cross section and strongly interfere with the Primakoff amplitude. Now, a simple model for the hadronic contribution, based on vector meson dominance (VMD), has been formulated by the theory group in Mainz, which allows to include this contribution in the cross-section estimation. Despite the fact that the model needs to be refined, in order to accurately analyze the cross-section data and extract the TFF, it gives a sufficiently reliable estimation for the purposes of a feasibility study. The main background process for the measurement, which is the incoherent electroproduction of pions on the single nucleons of the target, has also been estimated with a similar VMD model. This background can be suppressed kinematically to some extent, because the knock-out nucleon will have a larger recoil energy than the recoil nucleus in the coherent production. This suppression needs to be studied with detailed simulations, but for now the full background cross section is taken into account.

From these calculations, run time estimates were obtained. For a determination of the cross section with 1% statistical uncertainty about 170 hours of beam will be needed at the smallest Q^2 of 0.01 GeV^2. With about 1000 hours of beam, the 1% accuracy can be extended up to 0.03 GeV^2, while at 0.06 GeV^2 the statistical uncertainty would be about 3 %.

The detector construction activities are proceeding. In October 2019, a production readiness review (PRR) from the PANDA Collaboration took place at Mainz for assessing the status of the submodule series production, which was judged very positively. Almost all components needed for the series production are either delivered, ordered, or being manufactured. The major deliveries have been the shipping of all needed PWO crystals from Gießen to Mainz, the mechanical components for the equipment of the crystals with APD and preamplifier, the APFEL preamplifier boards, which are being assembled and tested at the GSI, and the sampling ADC boards, which were fully tested at Uppsala. The parts which are ordered but not yet delivered are the holding components of the submodules and the front-end boards with the signal driver, which are needed for the submodule production, because they will be glued to the aluminum feed-through holder of the submodule. Of the components which are produced in-house, about 4 carbon fibre alveoli per week are manufactured and there are in total 20 out of 50 so far. The Pt100 temperature sensor production is complete.

As soon as all components are available, the submodule series production can start. The procedure for the submodule mounting and testing has been worked out by constructing a first complete submodule and detailed written operating instructions have been compiled and approved by the collaboration during the PRR.

For the integration of the calorimeter into the A1 experimental hall, a new vacuum chamber is needed, in order to have a free particle path from the target to the detectors over the needed acceptance range. In order to use the available A1 target system, the new vacuum chamber needs to be designed with the usual A1 layout, which has a vertical cylindrical body, where the beam pipe is attached, and an upper and lower cap, through which the target services are fed into the vacuum volume. Only the cylindrical part needs to be manufactured with the same dimensions of the older chambers. Two 680 mm long aluminum hollow cylinders with a diameter of 0.5 m and a wall thickness of 25 mm are needed and have been ordered. They will be then machined at the mechanical workshop in Mainz.

KOALA@COSY

The PANDA Phase-0 experiment KOALA consists of two stages. In the first stage, KOALA@COSY measures the elastic proton-proton scattering differential cross section at very small momentum transfer. In a second stage, the same setup will be installed in the HESR as KOALA@HESR to measure the differential cross section of antiproton-proton elastic scattering at very small momentum transfer. The goal of this project is to provide the input necessary to achieve the desired precision for the absolute normalization of the luminosity measurements at PANDA. KOALA measures both the forward scattered particle and the backward recoil proton in coincidence in order to achieve a very high level of background suppression. The proton target is provided by the former ANKE cluster-jet target. The recoil proton is measured with the KOALA setup and the forward particle will be measured with the prototype of the PANDA Luminosity Detector. The measurements at COSY will provide high precision data extending into the Coulomb-dominated kinematic region in order to enable a comparison between pp to $\bar{p}p$ and to benchmark the respective hardware for FAIR.

KOALA recoil detector

The KOALA recoil detector was commissioned at COSY, showing that it can measure elastic recoil protons with nearly no background down to a kinetic energy of T=600 keV. In order to cleanly measure the recoil protons with even lower kinetic energy, it is needed to suppress the hadronic background rate near polar angles of 90° by implementing a coincidence with the forward scattered particle. A first measurement with a fast plastic scintillator telescope for the forward particle has been performed in 2019 at a series of beam momenta. As a highlight, this experiment achieved a coincidence measurement, enabling the recoil proton to be measured without background down to below T=400 keV. The overall evaluation of the performance will be gained after the full data analysis.

Luminosity Detector prototype

The LMD prototype is in preparation. The mechanical part of the system is ready. The vacuum box and also the support/cooling structure of the sensor modules has been tested extensively. The automation of the vacuum system and of the linear shift mechanism is proceeding and is expected to be ready soon. The MuPix8 sensors and the DAQ system for the readout of the sensors were tested at several beamtimes at COSY with the MuPix8 telescope with four sensors in a row. The complete sensor (all three sub-matrices) are working properly. During the DAQ test it turned out that the firmware for the configuration and readout of the MuPix sensors does not work together with SODAnet, the common experiment clock for PANDA. Since the TRBv3 FPGA board (HADES) is only able to readout four sensors in parallel, in the final setup it will be replaced with a new board based on the Kintex7 FPGA. For the KOALA@COSY experiment the Kintex7 evaluation board will be used. The first test with the new DAQ system using COSY beam is planned for spring 2020. At the end of 2020, all 16 sensors of the LMD prototype will be tested in COSY beam. In summer 2021, the KOALA@COSY setup will test the coincidence of signals in both the LMD prototype and the recoil detector. Concurrently, the electronics for serving the sensors and transporting the readout frames to the DAQ system will be finalized. In addition, the assembly of the sensor modules will be developed and standardized for the production. For doing this, a clean room with a bonding machine and a testing facility was setup in 2019. Also, simulation studies are ongoing to be able to extract the differential elastic cross section.

PANDA cluster-jet target at COSY

The PANDA cluster-jet target including the beam dump has been installed at COSY in order to test the performance of the target for later operation in HESR in as realistic conditions as possible. Major aims of this work are the investigation of the beam-target interaction, the

optimization of the target properties as well as the study of accelerator beam properties and vacuum situation as a function of the target settings.

During 2018, the cluster target was successfully brought into operation and stable target beams with target thicknesses of about 10^{15} atoms/cm^2 were achieved. In 2019, two experimental weeks enabled detailed investigations on the beam-target interaction with and without using the stochastic cooled and/or the COSY barrier bucket (HF). Measurements without beam cooling and COSY HF allow for energy loss measurements in the target via Schottky frequency shift measurements. These data in turn enable the (effective) thickness of both the target and the residual gas background to be measured. Using both beam cooling and COSY HF enable information about the HESR beam quality to be determined, especially since several components of the HESR stochastic cooling elements are installed at COSY.

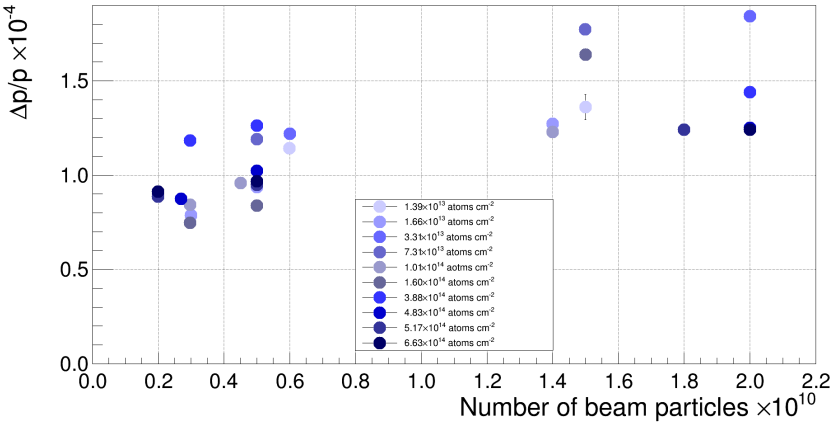

Figure 9: Relative COSY beam momentum spread for different target thicknesses as function of the number of stored protons in COSY.

A compilation of achieved beam quality data is presented in Fig. 9, showing the relative COSY beam momentum spread Δp/p for various target beam thicknesses as function of the number of stored protons. In addition, first data on the ion beam induced cluster evaporation have been collected, which give valuable information on the rest gas contribution of this effect. Due to the importance of these studies, new more detailed measurements will be performed in upcoming beam times. These will include considerably higher target thicknesses of $\rho \geq 2 \cdot 10^{15}$ atoms/cm^2, much larger cycle times (HESR conditions), and using an independent Schottky readout system.

General Project Management

Reporting campaigns

Reporting campaigns on a regular basis throughout the year have been conducted by the TC team collecting input from all PANDA system managers and were completed delivering all updates for a series of reports for FAIR AFC, Council and Management.

A new web interface has been created on the PANDA web to easily facilitate updates of milestones as well as the progress score of each system. In addition, the risk register files were updated as well.

FAIR L1 Workshop

The annual workshop of the FAIR project lead team took place Sep 16-17 at Bad Homburg, with the main objectives being the successful implementation of project review recommendations and Council decisions towards MSV.

In this workshop we dealt with project management topics, in particular scheduling, reporting, budget planning, as well as with topics of quality assurance, site management and pre-assembly and the current plans for the developments of the GSI campus.

Further topics concerning technical integration were addressed in a follow-up meeting and included alignment strategies, certification of conformity in view of the general operation permit and the development of the personal access system for beam areas at FAIR.

Clickable PANDA Detector

An interactive way of presenting our PANDA detector has been created as shown here: https://panda.gsi.de/panda.

Integration

The planning of the PANDA hall has resumed and progressed in coordinated efforts with the architects, the civil construction team and FSB team.

Technical requirements and the needs of all sub-detectors in the experiment have been communicated in order to optimize the hall construction and layout and the technical building infrastructures planning, such as service routing for technical gases and gas piping, pressurized air, and cooling water.

Services

A new envelope contour was prepared as input for further service routing planning to designate PANDA devices and needed service routing space for the devices.

On July 1 a first Lean Construction Management (LCM) workshop took place to coordinate the installation of all technical building infrastructures within the hall along with the installation needs of the PANDA experiment and the HESR accelerator.

One part of the services routing will be taken over by the planners of FSB, including gas pipes, the dipole supply cables and the Helium pressure line. The routing to the detectors will start from standardized patch panels, one for the target spectrometer and one from the forward spectrometer, which will be reached by high-quality stainless-steel piping from the supply area and the gas storage. A scheme of all needed gases and their logical routing was prepared as input for the planners.

The planning of mains power distribution and cooling services in the PANDA hall was aligned w.r.t. several principal power consumers like magnet supplies and detector cooling plants and the numerous racks placed in the counting house floors and around the spectrometers in the experimental area.

For the supply of the superconducting solenoid with liquid Helium a cryogenic plant is projected in the PANDA building. The budget is part of the funds for the HESR machine under responsibility of the team at FZ Jülich and the work on specification and tendering of the plant is coordinated together with the cryogenics group of FAIR at GSI and the PANDA coordination team.

The component data base serving as input for the planners of the hall's technical infrastructure has been updated accordingly.

Radiation protection

Reassessing the radiation protection category of the PANDA beam area with a simplified model of the experiment as input for more precise FLUKA simulations of a more realistic scenario led to a change request to the civil construction team. The change request was approved on the basis of newly reduced radiation protection requirements for the PANDA beam area allowing for a more simplified ventilation of the area leading to significant savings and also a simpler handling and sealing of the movable shielding wall.

Layout

Several requirements from the side of the architects were coordinated with the needs of the experiment to optimize the hall construction and layout. Examples are the gangways around the maintenance area, protection railing at pits and thresholds, the operation of the main goods gate and the radiation protection ceiling of the beam area.

The placement of the person locks for radiation protection was discussed with FAIR Site & Buildings (FSB) and the radiation protection department. There are two locks foreseen, one leading into the beam area, which will be fully closed during beam operation, and another leading into the maintenance area which has to be controlled as some radioactivity can be carried out from the beam area when the spectrometer moves to maintenance position.

Installation

A great deal of progress has been achieved in planning the PANDA installation at the sub-detector level as well as in the design of platforms and support structures for installation and maintenance.

At a two-day workshop at GSI on Feb 18-19, 2019, the installation concepts and procedures of each sub-detector were presented and discussed as well as structural mechanic interfaces among several sub-detectors, such as the new design of the CSF.

Notably, the new concept of the Central Space Frame (CSF), designed at GSI, integrates the mechanical support for the MVD and the STT, and additionally provides the necessary support of the heavy services for the MVD placed around the beam-pipe upstream of the interaction point. In cooperation with the updated design of the Barrel DIRC mechanics, this new CSF design is now mechanically integrated in the cylindrical support structure of the Barrel DIRC. As for the CSF material besides carbon fiber composites, aluminum is also being examined.

PANDA installations are planned in line with the framework of installation on-site at FAIR. Installations are planned to proceed in parallel to the installation of the technical building infrastructure to be coordinated in weekly and daily Lean Construction Management (LCM) meetings to avoid clashes and to optimize the available time. All components are to be readily

prepared for installation and completely documented in the Product Lifecycle Management system (PLM) including work descriptions and hazard analysis.

PANDA installation planning involved the complete collection of individual installation procedures, the formulation of individual installation schedules is required as well as the specification of needed resources.

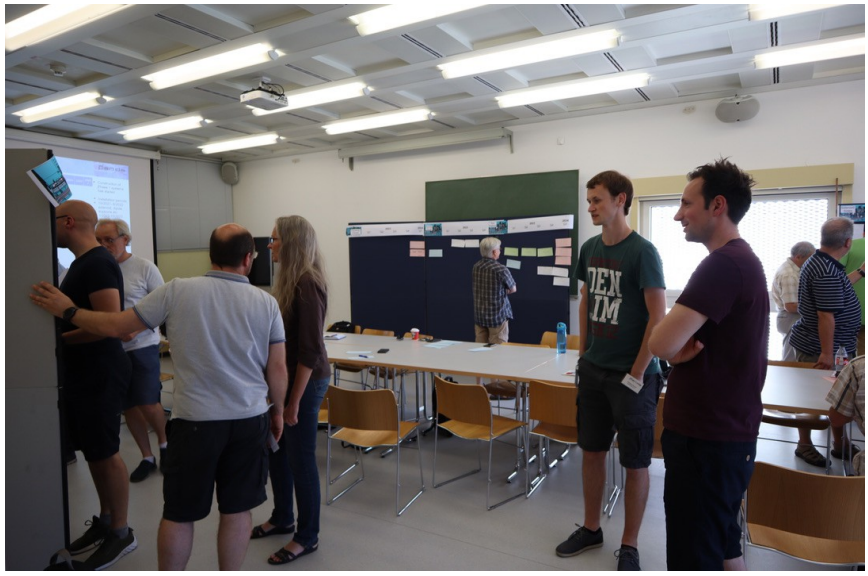

Figure 10: Hands-on installation workshop.

A dedicated interactive “pin-board” workshop took place on 28-June-2019 with all system managers and colleagues involved in the installation of their sub-detector in the TS, organized by the coordination team at GSI.

The workshop focused on the specific installation requirements of each system in the TS with the aim the alignment of schedules and resources, in order to further coordinate parallel activities during the installation phase, such as the integration planning of tooling, the temporary platforms and auxiliary structures.

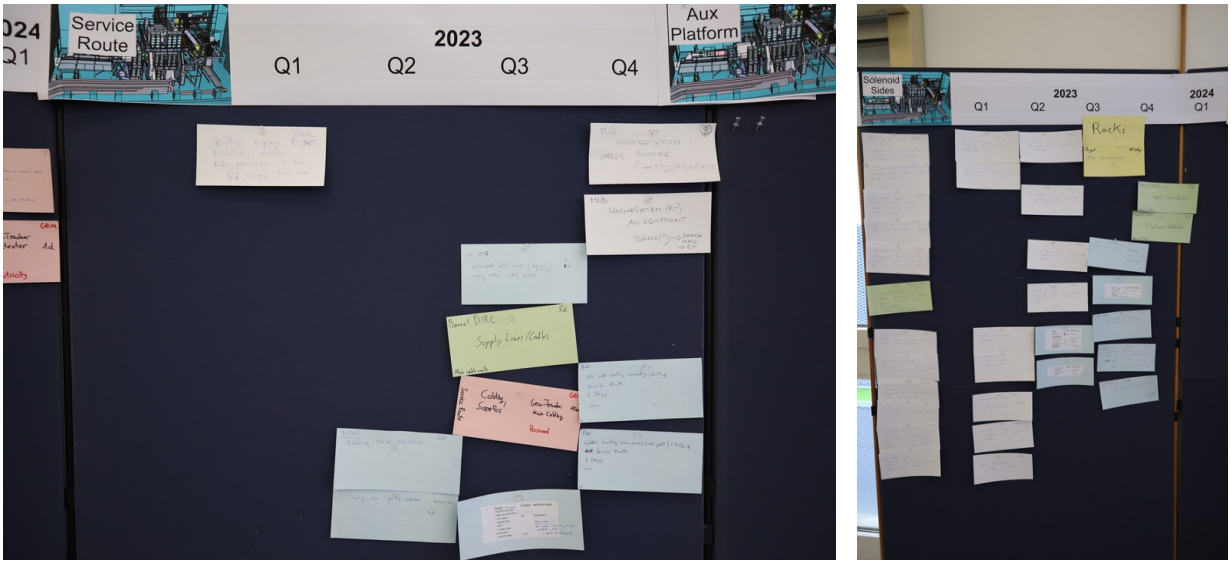

Figure 11: Planning pin-boards. Classical methods still work excellent.

Ten pin-boards were mounted denoting ten locations in the PANDA hall for concurrent installation work. On top of each board a time-axis was given together with a picture of the location. Each individual installation step was denoted on a moderation cards with title, duration and needed resources.

Each system responsible placed the previously prepared cards on the appropriate locations at an approximate timeline following the system's production schedule. After all cards of each system were placed the individual locations and also correlations between them were discussed one by one, leading to adjustments to the sequences and time-wise placements were

accomplished. A detailed photo protocol of the results on the pin-boards was made and the cards were collected to be able to reproduce the settings.

The outcome of this workshop was analyzed in cooperation with experts from the FAIR Project Management Office, correlated across the specified locations and systems and transferred into the overall planning frame of PANDA installation within the FAIR Microsoft Project Server. In addition, generic host-lab resources, in particular personnel for logistics, survey and cryogenics, were entered into the planning. The end date of the installation resulting from this much more detailed planning comes close to prior expectations leading to the start of overall commissioning without beam in spring 2024.

Support platforms

The layout of support and installation platforms in the maintenance position has been further refined and adapted to the needs of the sub-detectors and also taking into account safety relevant surrounding elements like railings and person locks.

A more detailed planning of infrastructures like support and assembly platforms, staircases, rack support consoles, the auxiliary platform and other items is ongoing.

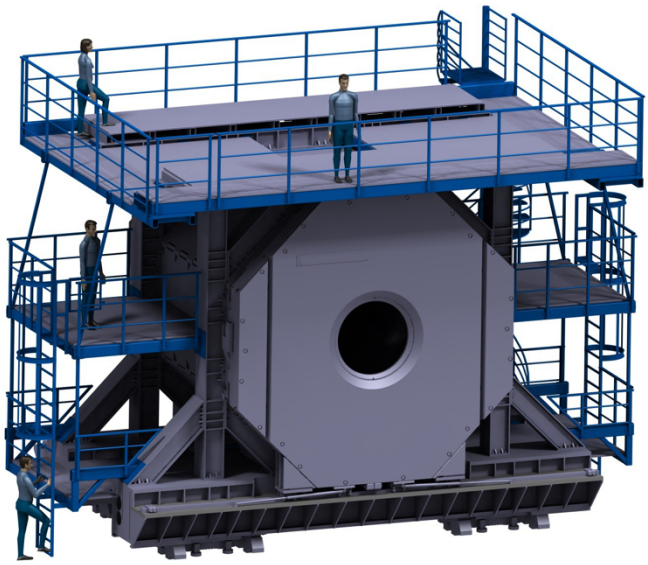

Figure 12: Support platforms around the magnet yoke.

Magnets

Solenoid

Major progress has been achieved by BINP with the completion of all octants of the yoke produced and machined. Also, the support beams have been produced and are ready for usage. Preparations for the first barrel test assembly are on-going at the subcontractor SET.

Figure 13: Production of yoke octants completed.

A new technical device was designed by SET to correctly align all octants with respect to each other. The complex first assembly requiring additional tooling for shimming and adjustment is being prepared as well as the special area with a flat surface exceeding the initial requirements.

This first assembly is planned without the yoke doors, which will be added as soon as the alignment of all octants is done. After the full assembly the whole yoke will be transferred to BINP where a suitable location has been identified to continue assembling the solenoid magnet.

Figure 14: Single yoke octant

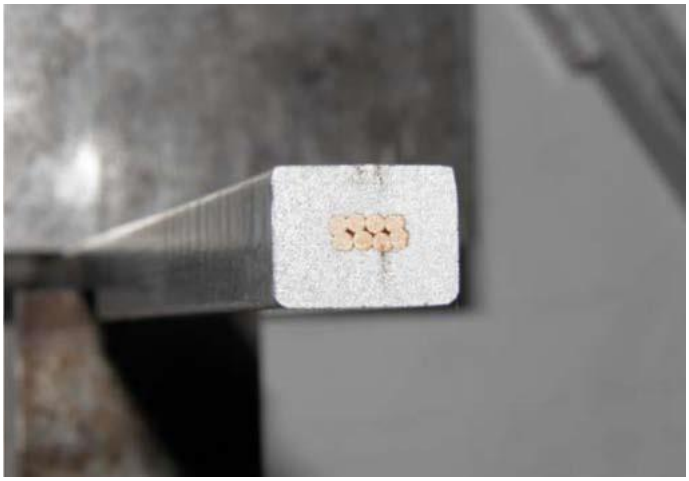

Regarding the superconductor the developments of the extrusion technology at the company Sarko have been successful as demonstrated in reliable production of conductor samples with results satisfying in all respects.

Figure 15: Conductor sample produced for PANDA.

The tools for the coil production are designed and are currently in preparation. First tests of the tooling are planned with a simple Aluminum conductor.

Several review meetings took place at GSI with experts from CERN and the FAIR cryogenics group on the design of the proximity cryogenics, control dewar, thermal shield, the vacuum scheme and instrumentation.

Figure 16: Sample coil winding from Aluminum.

Dipole

The detailed design of the dipole magnet is progressing at BINP. Simulations of the static and seismic stability of the support are being prepared along with a functional 3D model as the basis for all production drawings.

Upon completion of the intermediate design report the contract for the production of the magnet will be signed.

Targets

Cluster Jet Target

The prototype Cluster Jet Target and the beam dump have been used *successfully throughout* the year at COSY, in several beam times for a multitude of target design studies and also for beam operations studies relevant also for the HESR.

In particular noteworthy are the beam life-time studies for HESR parameters, with beam momentum of e.g. 3.2 GeV/*c*, studies of high target thicknesses and the use of the cluster jet target for accelerator studies of stochastic cooling and barrier bucket. The beam time included also tests to reach PANDA cycle times of e.g. 1800s and ion beam induced cluster evaporation studies as well as data quality studies.

Further R&D activities are continuously pursued at the test station at WWU, Münster, on nozzles, pumps and other elements for further target developments including simulations of operational parameters and their comparison with data.

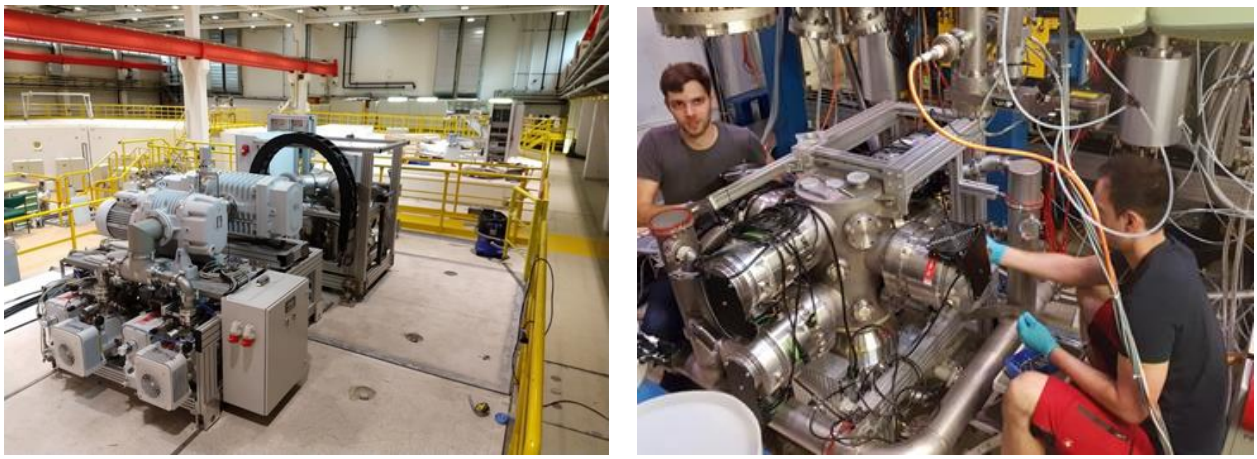

Figure 17: The source of the cluster-jet target in its testing position in the COSY storage ring at FZ Jülich (left). Preparations for the beam dump (right).

Vacuum and residual gas

A recent development concerns simulation of the regarding the rest-gas in the beam-pipe close to the interaction point (IP) in PANDA, with efforts to minimize adverse impacts, such as to use a cryo-pump within the beam line and changes to the beam pipe diameter near the IP.

Pellet Target

The pellet target prototype at ITEP has made major progress in all technical aspects towards an operational system with the target cryostat, the scattering chamber and dumping system, the gas supply and palladium purifier systems, the vacuum system and parts of the monitoring and operations system.

Figure 18: Pellet target prototype at ITEP.

On-going are the developments on the adjustment systems for nozzle and sluice, and automation of the new diagnostic system. Several important measurements and long-term stability tests have been performed, and the release of the TDR is planned in 2020.

Tracking

Micro Vertex Detector (MVD)

A further batch of strip sensors arrived at Giessen and the qualification and acceptance showed a satisfactory yield. Concerning the mechanics staves for strip barrel produced at IKV – Aachen and checked at FZ Jülich meet the requirements, yet the production process optimization is still necessary. Due to difficulties in the mounting process the strip disc design is being optimized. Irradiation tests of all mechanical components are planned.

At Torino, the development of ToAST ASIC, the new full-size prototype for the strip readout has progressed with submission scheduled for 2020. Also, at Torino, the characterization of 110 nm UMC technology for upset effects has been completed.

Concerning the pixel part of MVD, discussions on the possibilities and challenges if HV-MAPS devices could be employed in the MVD pixels region for the Day-1 setup have started and continue. A preliminary idea to use strip discs has also been proposed.

Straw Tube Tracker (STT)

All the straws for the STT have been produced and the module production is being prepared including the assembly of one sector in the prototype frame. Operational controls of gas, HV and LV systems via EPICS has been provided by IFIN-HH Bucharest.

Data from beam times at COSY with STT modules have demonstrated that the required separation power is well achieved and with straw calibration and tracking methods developed in FZ Jülich including energy loss determination.

A major milestone achieved is the in-kind contract for the production of the readout electronics for the Straw Tube Tracker and Forward Tracker signed between FAIR and Poland, that is the Polish Shareholder of FAIR and the in-kind provider AGH University of Science and Technology, Cracow.

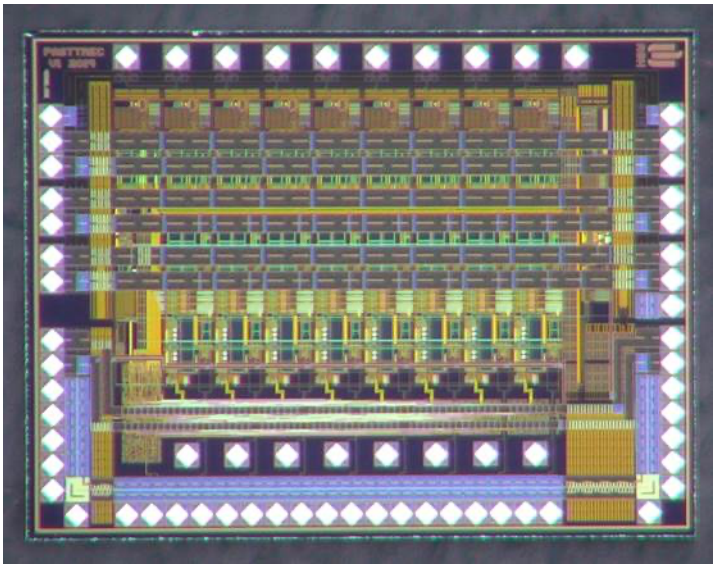

Figure 19: PASTTREC ASIC.

Figure 20: STT/FT FEE board.

The first, most urgent task is the procurement of the readout ASIC PASTTREC developed in Krakow. In parallel the development and optimization of the printed circuit boards shall take place. This will be followed by the production of boards and further digital electronics.

Both the STT and the Forward Tracker (FT) groups have Phase-0 activities contributing tracker stations based on PANDA straw tube detector technologies to the HADES experiment at GSI.

The tracker stations STS1 and STS2 built by the FZ Jülich and JU Cracow groups respectively, are equipped with the PASTTREC ASIC readout electronics, and have been tested in beam times at COSY.

Additional mechanical support structures have been produced for the installation of the PANDA tracker stations in HADES which are planned to be used in the forthcoming beam times at GSI.

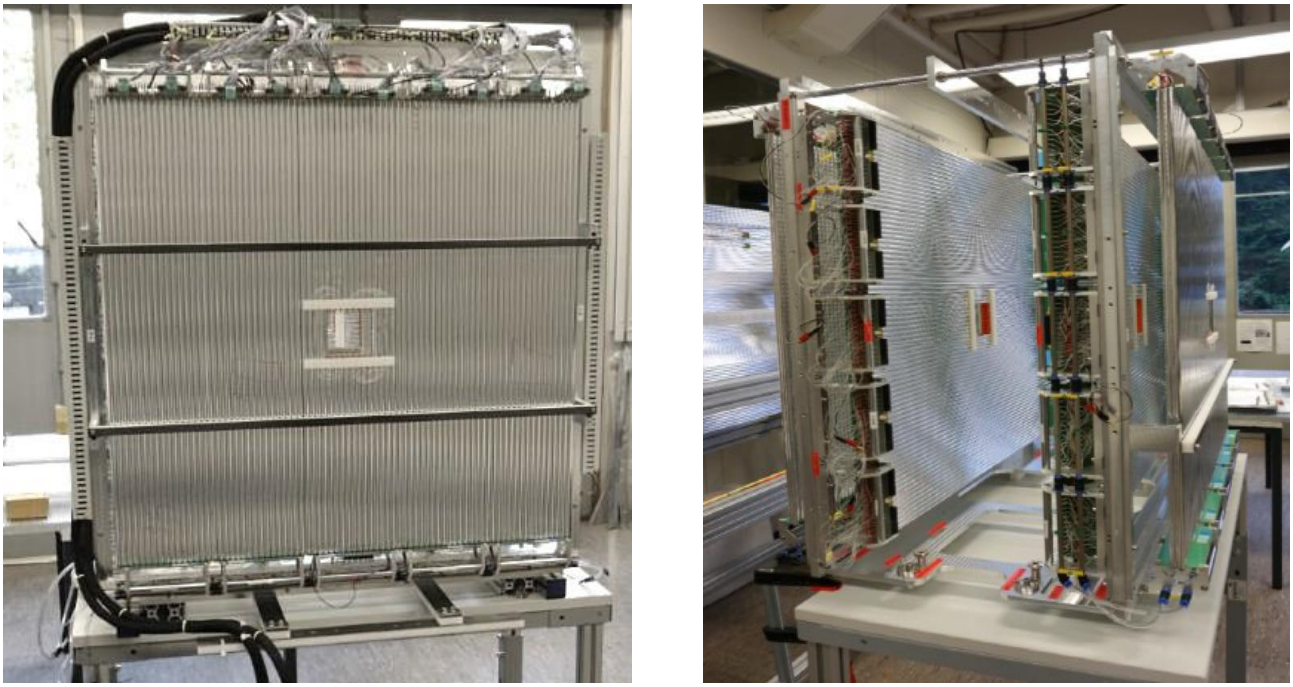

Figure 21: Single and multiple STS planes.

Figure 22: STS installation at HADES.

Gas Electron Multiplier (GEM)

The GEM foils produced by TECHTRA have been received and prepared for QA tests at GSI, including development of an in-house etching process for the readout structures. Unfortunately, a fire at TECHTRA has put production of large foils on hold until the end of 2019.

Concerning the GEM detector mechanics, the base data have been re-worked and updated, including the installation concept.

Regarding readout electronics the STS-xyter or the Hit Detection ASIC were considered. The readout option developed around the HitDetection ASIC from the GSI electronics department has been tested in-beam at GSI jointly with the Super-FRS GEM TPC prototype assembly and the data are being analyzed.

Further beam tests are planned jointly with the mini-CBM setup at GSI and completion of the GEM Tracker TDR is planned in 2020.

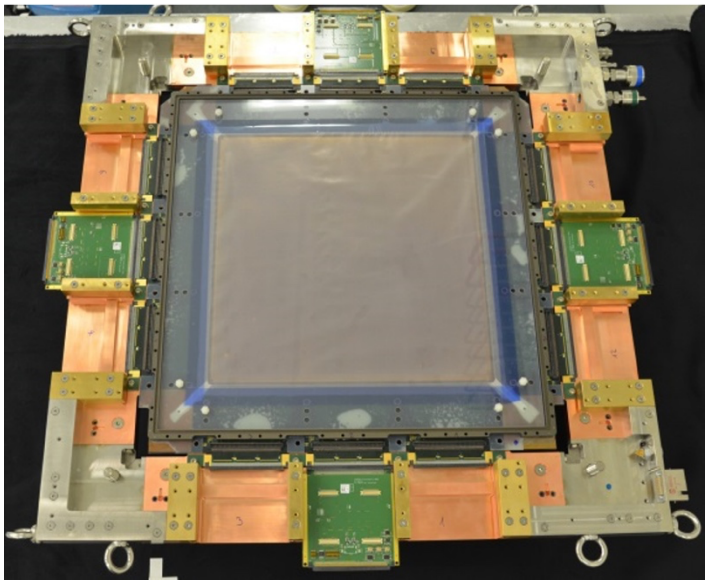

Figure 23: GEM 2D Demonstrator.

Forward Tracker (FT)

A Forward Tracker setup of eight double layers in-beam at COSY this year has shown very promising results of high detection efficiencies across the whole range of the operational parameters. Following the ratification in March 2019, colleagues at SLRI, Thailand have been contributing controls software for the FT, specifically for the LV, HV modules and the gas system (flow meter, pressure gauges). Systematic aging studies of straw tubes have been conducted and the results obtained analyzed to identify the source of aging, Further tests are planned to devise mitigation measures.

Figure 24: FT Module production.

The possible use of LHCb Outer Tracker (OT) Planes as FT5&6 in PANDA has been pursued strongly at GSI.

A transport container from CERN has arrived at GSI with all available spare straw-tube modules of the LHCb OT, including handling tables and mechanical tools and several sets of readout electronics. The spare OT modules have been inspected and their dimensions measured. The work package related to the design and construction of mechanical frames for PANDA has been discussed and accepted by our colleagues in Thailand.

In addition, the design of an interface board to the PANDA readout electronics has started at GSI.

Figure 25: Delivery of LHCb Outer Tracker Modules to GSI.

Luminosity Detector (LMD)

The TDR of the LMD has been accepted by the FAIR ECE, following the submission of a revised version with detailed answers to the questions of the reviewers.

Many technical aspects of the LMD have progressed significantly, such as mechanics, cooling and electronics as well the status of sensor characterization and data acquisition and controls.

Various components of the LMD, such as the sensor MuPix8 were tested in beam times at COSY four-layer MuPix8 telescope, and in the laboratory, and found to perform well within the requirements for PANDA.

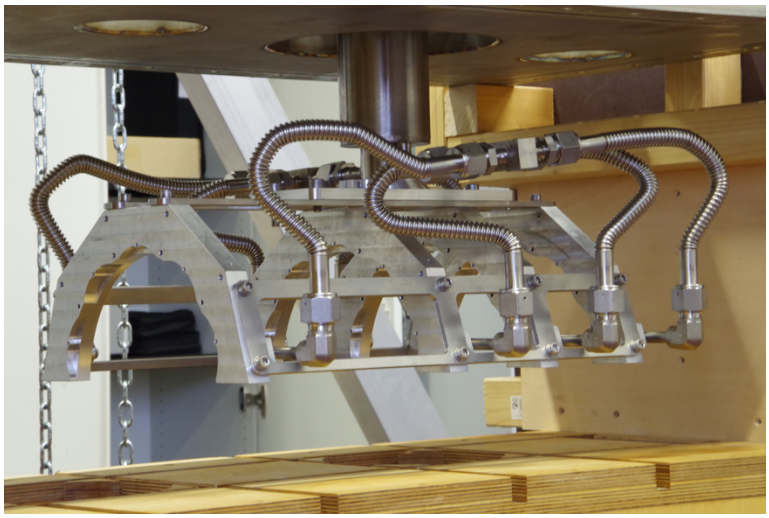

Figure 26: Prototype of the Luminosity Detector (Mechanics).

System tests, such as those for mechanics and cooling of a complete half detector setup with copper dummies and resistors instead of diamond wafers and silicon sensors, showed that stable operational conditions can be achieved throughout the lifetime of PANDA.

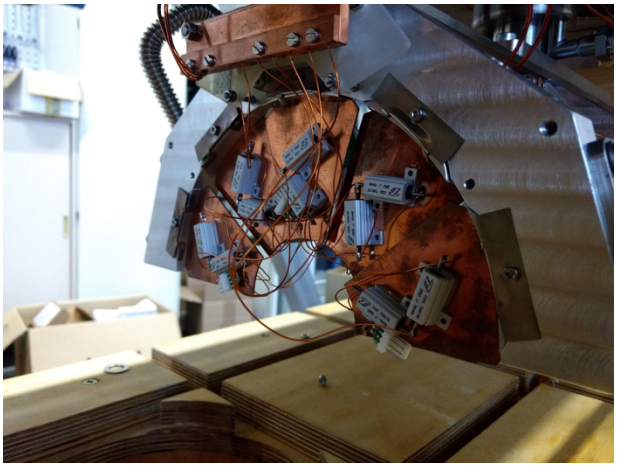

Figure 27: LMD Half plane system tests.

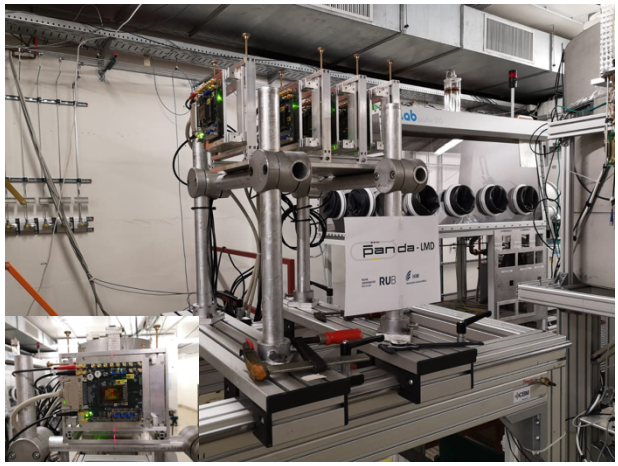

Figure 28: LMD Four-layer MuPix8 telescope.

Electromagnetic Calorimeter (EMC)

Forward Endcap EMC

The construction of the Forward Endcap EMC (FWE-EMC) is in a very advanced stage. All VPTT sub-modules have been produced and tested, ready for installation.

The APD sub-module production started following a PRR by the Technical Coordination concerning the APD mass-screening, the matching and the sub-module assembly at Bochum University. Notably, two climate chambers operate on a permanently, with automated procedures achieving a screening throughput of 600 APDs per week. APD irradiation and annealing takes place at the “Strahlungszentrum Gießen” using a dedicated PCB design for high throughput and safe transport.

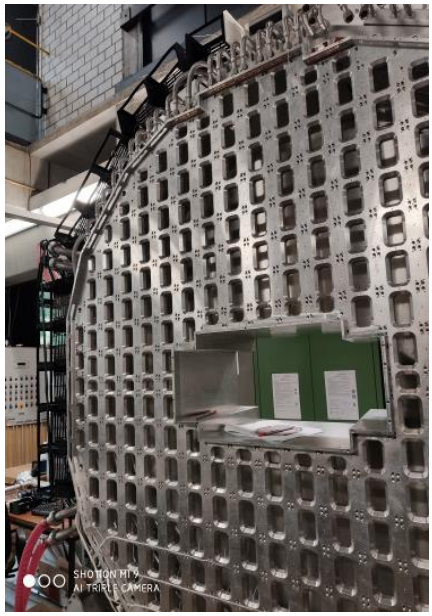

Figure 29: Forward Endcap EMC holding structure in assembly position.

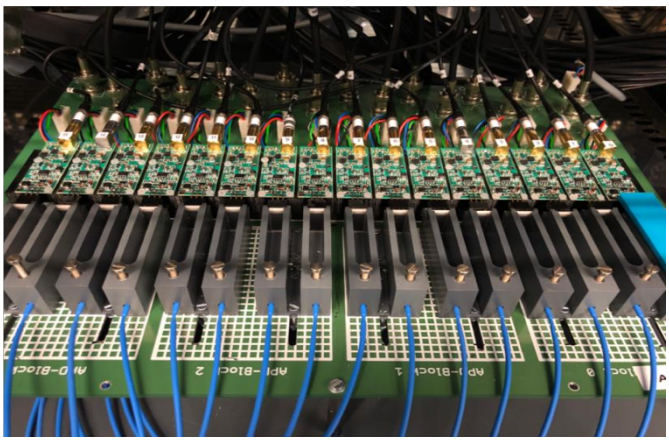

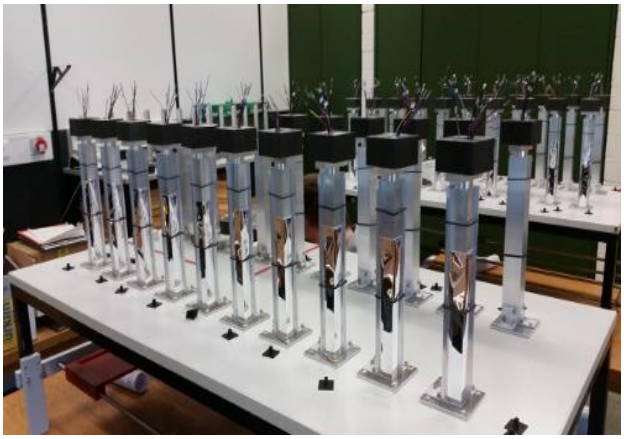

Figure 30: APD sub-module production. APD gluing on crystals (left) mass screening (right).

Several QA checks are part of the sub-module production chain and further tests are conducted on the completed sub-module at Bonn University. All 250 front-end Sampling-ADC boards have been produced and checked at Uppsala University.

Continued progress made on the cooling circuitry and piping as well as on the SADC crate layout placed on the frame has defined the routing of cabling paths.

At FZ Jülich the support structures, the mounting arm and the local readout unit are prepared for the pre-assembly of the full FWE-EMC.

Backward Endcap EMC

Based on the successful results of the sub-module prototypes in the MAMI beam times, the sub-module design has advanced towards series production for the complete Backward Endcap EMC. The Phase-0 activities at the A1 spectrometer at MAMI continued with the more advanced prototypes. Notably, the Alveole mechanical design allows to easily modify the Phase-0 layout to the PANDA layout.

Preparations for series production of sub-modules have started and following the PRR at HIM, the procurement of parts and components have advanced steadily, with the series production planned in 2020.

Figure 31: View of a single crystal assembly (left).

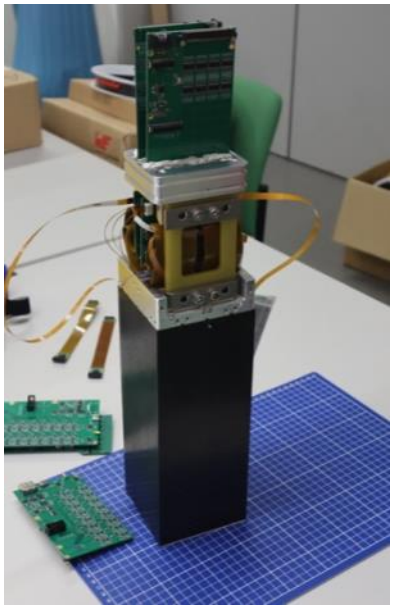

Figure 32: Preparations of BWE EMC module assembly (right).

Barrel EMC

At IHEP Protvino all alveoli packs of eighteen different types for the whole barrel, all rear and front inserts and all intermediate plates have been produced and were delivered to the slice assembly site at Giessen University.

The First-of-Series slice is almost complete, with some adjustments due on the cooling and thermal insulation, on a few backplane re-designs and light-pulser fiber couplings. Inspections on the stiffness of the support beam showed acceptable results.

Also, the revised version of the Serial adapter ASIC for HV regulation fulfills well the operational requirements.

Crystals have been produced throughout the year at the company Crytur (Czech Republic) of high quality, matching the previously produced batches of BCTP in Russia. Completion of crystal production for the second slice is expected early 2020 and production shall continue until all slices of the Barrel EMC are complete.

Figure 33: First of Series slice for the Barrel EMC and support beam (left). First of Series slice for the Barrel EMC, front-end electronics view (right).

HitDetection ASIC

Two test chips of the HitDetection ASIC development at GSI with full functionality for the readout of the Barrel EMC were submitted in July. A setup for testing the ASIC has been built at GSI and a second test station is being prepared for HIM to conduct a series of tests on the HitDetection ASIC. Submission of the full version is planned for spring 2020 after the results from the tests are taken into account.

Forward Shashlyk Calorimeter

At IHEP Protvino progress has been made on the HV board for the photomultiplier tubes of the Forward Shashlyk Calorimeter. The design based on a Cockroft-Walton voltage multiplier now includes also an ADC for HV monitoring.

Preparations for contracts to manufacture components have started by updating technical parameter specifications.

Detectors for Particle Identification (PID)

Barrel DIRC (Detector for Internally Reflected Cherenkov Light)

The Barrel DIRC group has made significant progress in the tendering process at GSI for components of high costs and long lead-times, which are the fused silica radiator bars and the MCP-PMTs.

Offers from several vendors world-wide have been considered, of which one vendor (Nikon Corp.) has been awarded the contract for the fabrication of the fused silica bars in Sep. 2019. Pre-production has started and the delivery of first bars is expected early 2020.

The call for tenders for MCP-PMTs is still ongoing. The bidding vendors are asked to provide two engineering samples each for the technical qualification at GSI and FAU, Erlangen, leading to a decision on the selection of the vendor.

A QA test-stand in the DIRC optical laboratory at GSI has been developed to study bar casing materials and possible impacts on quartz bar surface quality.

Further activities included testing prototypes of lenses, optical couplings and the DiRICH readout electronics and also significant progress on the mechanics.

The successful Phase-0 program continued with commissioning the second half of GlueX DIRC with the GSI team again involved in calibration, reconstruction, simulation and performance studies.

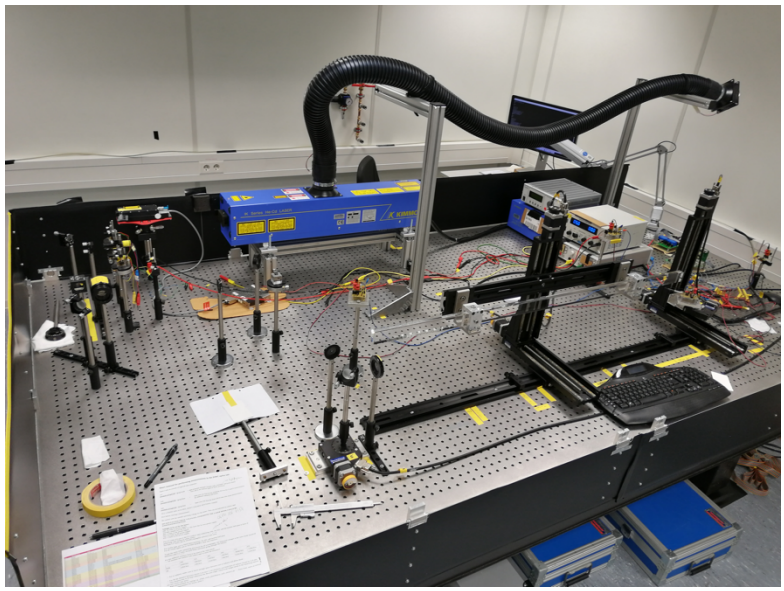

Figure 34: Laser setup in the DIRC Optical Lab at GSI with internal reflection precision < 0.1%.

Figure 35: Pollution setup in the DIRC Optical Lab at GSI to study materials and surface impact on radiator bars.

Endcap Disc DIRC (EDD)

The Endcap Disc DIRC TDR has been reviewed by the FAIR ECE and approved in Nov. 2019. This paves the road to obtain funding for a first-of-series version of a full-size quadrant of this new detector concept in PANDA, possibly already for measurements with first beam.

The Cosmic Test Stand at Giessen University has been further developed for QA measurements of a quadrant including tests with the readout electronics, the TOFPET ASIC by PETSys. Concerns of the limited space for the readout devices and services led to studies of changes in the layout with the respective performance evaluations being in progress.

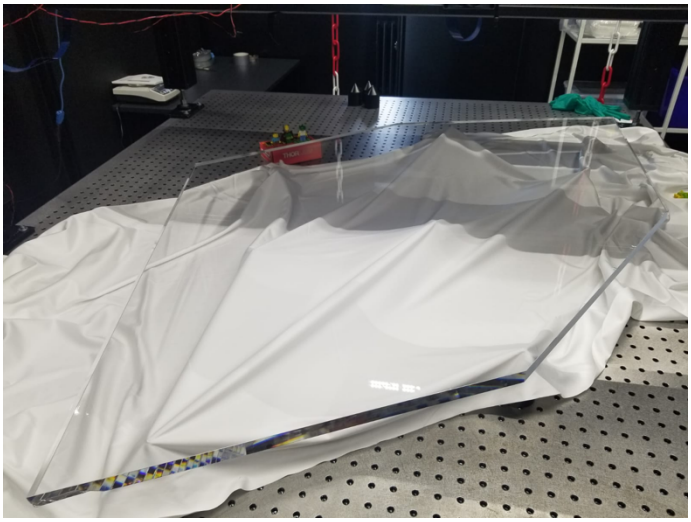

Figure 36: Full size (one quadrant) radiator plate prototype.

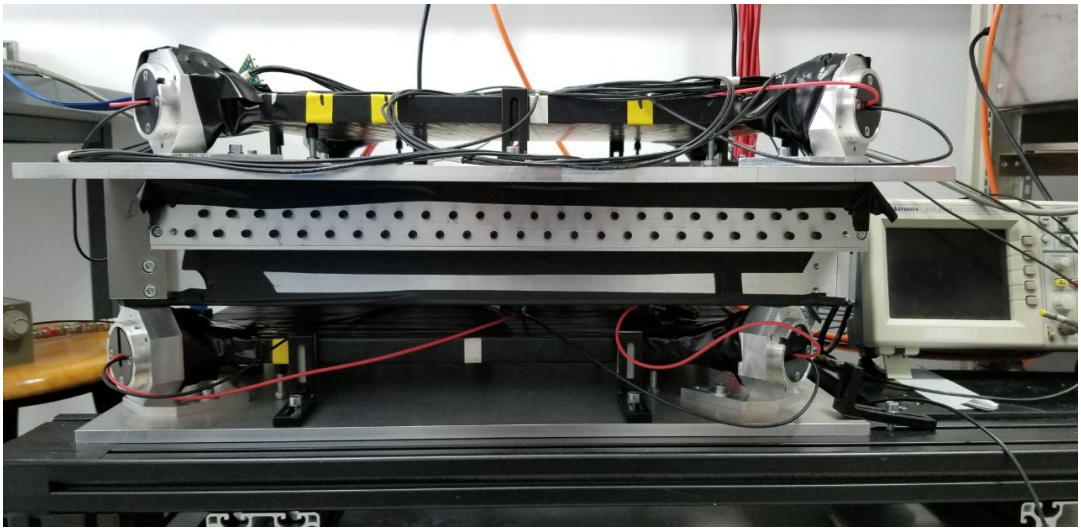

Figure 37: Cosmics test station being setup at Giessen.

Forward RICH (FRICH)

Beam tests with an advanced prototype of the FRICH took place with an electron beam (3 GeV) at VEPP, BINP in June 2019. The prototype consisted of stacked two-layer aerogel radiators, flat mirror, and four MaPMTs and two different readout systems, the DiRICH & the TRB3.

Test beam results showed the onset of Cherenkov rings, and include single photon resolution and number of photoelectrons with first analyses indicating that both fulfill the required π/K separation power. More detailed studies and comparisons with simulations are ongoing. Further developments of the optical laboratory at NSU allow QA measurements on components like mirrors and PMT scans. The FRICH TDR writing process has started and a release is planned in 2020.

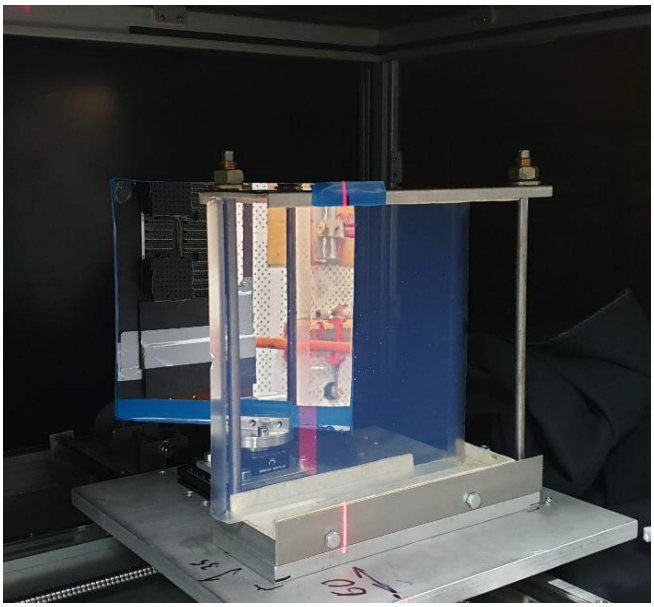

Figure 38: FRICH beam test setup, aerogel stack & mirrors (right), and MaPMTs & readout electronics (left).

Barrel Time-of-Flight (TOF)

Design changes to several Barrel TOF components have been proposed aiming at reducing signal attenuation loss, increase mechanical stability of modules, ensure light tightness and ease of construction and maintenance.

The design changes concern the rail board and the super module, and the shape of the plastic scintillators.

Prototypes are being produced to validate the new design and minimize adverse impacts due to an increase of the material budget. The analysis of the CERN 2018 beam data has made good progress and is almost completed.

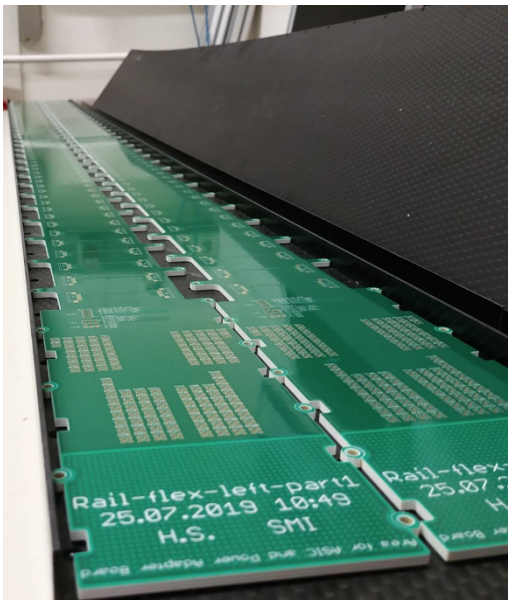

Figure 39: Barrel ToF prototypes: Railboard PCBs in carbon fibre enclosure.

Forward TOF

The Forward ToF system is part of the Russian contributions to FAIR and had the TDR approved by FAIR in 2018. At PNPI St. Petersburg, the lead institute, test stations have been developed to measure technical characteristics of scintillators slabs and PMTs to compare between different types and models.

Figure 40: FToF laboratory at PNPI for measurements on scintillators and PMTs with readout electronics.

A calibration system based on a pico-second laser-pulser has been set-up for mass production tests of slabs and PMTs, and performance simulations are ongoing.

Figure 41: Test setup with a stack of several scintillator bars at PNPI.

Muon System (MUON)

In the target spectrometer the segmented yoke of the solenoid is instrumented with chambers for muon identification and the FS has the Muon Range System for muon detection, both using drift tubes with wire & cathode strip readout developed at JINR Dubna.

The large prototype so far used in many test beams at CERN has been moved to the COMPASS area taking cosmic runs.

First observations of muon tracks with the newly developed FPGA/Artix7 read out has been reported. The full scale (192 channels) VME unit based on FPGA/ARTIX7 chip was commissioned and has demonstrated expected performance. This FPGA will be used in the final muon system readout.

Geometrical models of the muon system parts are ready for integration into PandaRoot. Digitization / pattern recognition studies of hadrons and muons of previous beam data continue.

Figure 42: Muon system prototype at CERN.

Common Systems

Detector Controls System (DCS)

The DCS TDR has been formally submitted to FAIR on Aug 28, 2019 to be reviewed by the FAIR ECE.

Prior to the submission, the TDR went through the PANDA internal review, a procedure involving external experts to scrutinize the document. Recommendations and additions from the internal review were followed and implemented.

The DCS is based on Experimental Physics and Industrial Control System (EPICS), and shares expertise and developments with other experiments on-site, HADES, CBM and with the user community world-wide.

The DCS core team provides practical guidance and demonstrations, such as the use of docker images for the control of a power supply and continues the support of PANDA sub-detectors.

Data Acquisition System (DAQ)

Steady progress has been made towards completion of the DAQ TDR. At the annual PANDA DAQ-FEE workshop all technical aspects were discussed such as the Data Concentrator and the Burst Building Network, the Compute Nodes and possible alternatives and the synchronization network SODANET.

New groups from China and Germany have expressed strong interest to participate in the DAQ system.

The synchronization concepts have been validated in a beam-time with DAQ hardware prototypes available of two different sub-detectors.

The first complete DAQ TDR draft has been presented to the collaboration for comments before entering the PANDA internal review process, early in 2020.

Computing and Software

One essential part for a successful PANDA experiment is the simulation and reconstruction framework PandaRoot. Before the start of the experiment it is used to simulate the performance of the detector design, it determines the operation parameters of the different sub-detectors of the experiment and it is used to develop reconstruction and analysis strategies to be used once real data is available. After the start of PANDA, it will be the brain of the experiment which does the reconstruction of the detector data and performs the analysis stages to produce the results of the experiment. The development of the software is a huge enterprise which includes many different development steps.

One milestone reached in 2019 for the development of PandaRoot was the implementation of an (mis-)alignment procedure suitable for different sub-detectors.

Until now, detector and component misalignment had to be implemented by every working group at PandaRoot individually, leading to much code duplication and potential for errors. The specific order of position and misalignment application of each component was the responsibility of the detector classes, and by extension their developers. Because PandaRoot inherits from FairRoot, the same holds true for FairRoot.
Now, methods to easily misalign the detector geometry have been integrated into FairRoots `FairRunSim` and `FairRunAna` classes and are immediately available to all FairRoot users, allowing them to run comprehensive detector studies at misaligned components with minimal effort. The user can choose whether to misalign the actual working geometry and study the resulting effect on the detector acceptance, or to mimic misalignment by moving reconstructed hits before track reconstruction instead of detector parts. This way, only a single set of Monte

Carlo data has to be generated to study multiple misalignment types and magnitudes. Misalignment of individual components, component groups and entire subdetectors can be switched on or off individually. Both actual and mimicked misalignment only require the creation of misalignment matrices, homogenous 4x4 transformation matrices which describe a component's offset from its design position.

One detector strongly affected by the alignment accuracy is the Luminosity Detector. Therefore, it was chosen as a test example for the new (mis-)alignment methods. In hadron spectroscopy, the mass and width of many states are measured with the energy-scan method, which relies on precise knowledge of the luminosity. At PANDA, the Luminosity Detector will be built to measure the luminosity with 1 % accuracy for the energy scan measurements. The key studies during the development of the alignment procedure treat the effect of misalignment on the accuracy of the measured luminosity.

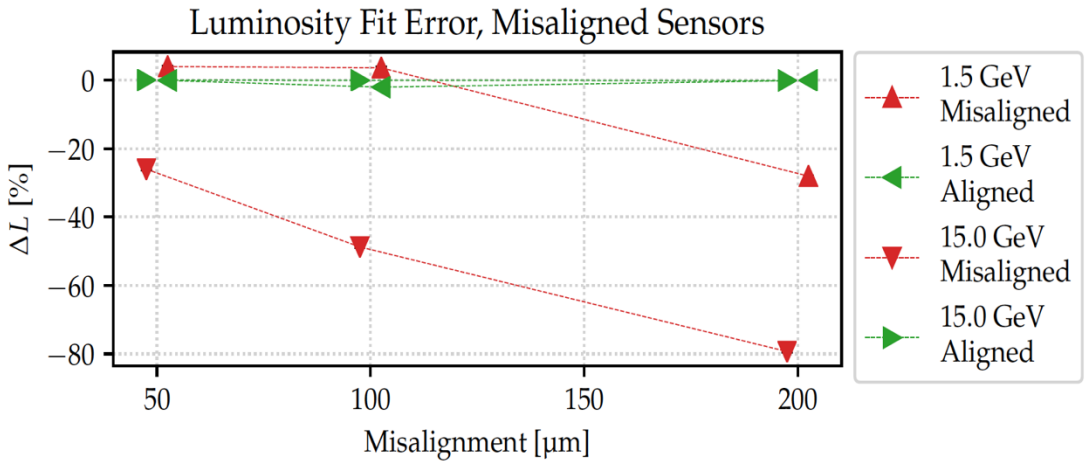

Figure 43: Error on the reconstructed luminosity for different misaligned geometries and beam momenta with and without correction.

Software alignment methods to correct that misalignment have been developed as well. Three algorithms to determine each components misalignment have been developed at and tested on the Luminosity Detector, utilizing principal component analysis for fast track fits and singular value decompositions for the assessment of misalignment. These alignment techniques result in a decrease of the luminosity fit errors due to detector misalignment from several tens of percent down to sub-percentage accuracy (see Fig. 43).

One important requirement for PANDA is the precise measurement of charged tracks which needs sophisticated algorithms for track finding and fitting which are one of the most demanding aspects in processing the measured data. Here important progress both with modernizing classical approaches as well as adaptive machine learning methods was made.

A significant milestone was the completion of the PzFinder, a set of algorithms to reconstruct the longitudinal track parameters of charged particles. It specifically focuses on the Straw Tube Tracker. While most straw tubes in this detector are aligned parallel to the beam pipe, 8 layers have an inclination angle of ±3° and thus allow the extraction of position information in longitudinal direction. This requires an alignment procedure of the drift circles in the straw tubes to a preliminary track fit which, however, introduces a spatial ambiguity to the determination of the longitudinal position. Three methods were developed to resolve this ambiguity: A combinatorial approach, a Hough transformation, and a recursive annealing fitting approach.

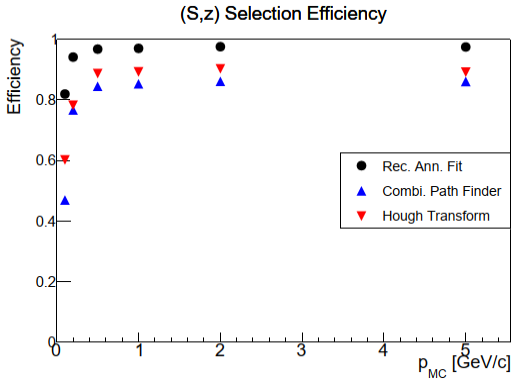

Figure 44: Selection efficiency of the PzFinder.

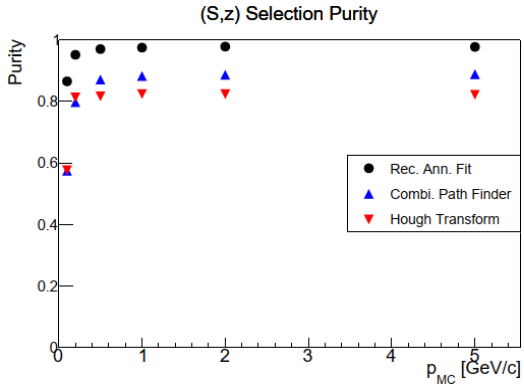

Figure 45: Selection Purity of the PzFinder.

The performance of the individual approaches has been studied using simulated muons in the expected momentum range of PANDA. The recursive annealing fit was found to perform best across all categories, including hit efficiency, hit purity, and momentum resolution. The former two of these are shown above. As can be seen in Fig. 44 and 45, the recursive annealing fit achieves a satisfactory 95 % efficiency and purity across a large momentum range. The PzFinder algorithms show promise both as a stand-alone reconstruction in the STT as well as in conjunction with the Micro Vertex Detector.

The purely software-based triggering system that PANDA will utilize, requires adaptations of the existing algorithms for them to be able to handle free-streaming data. This is addressed by the ongoing work on time-based track reconstruction, which made important progress over the last year. Several track finders are now able to accept time-sorted hits, including the `SttCellTrackFinder` and the `IdealTrackFinder`. The `SttCellTrackFinder` focuses on the Straw Tube Tracker and implements a cellular automaton-based pattern recognition and a track fitting procedure based on Riemann mapping. Since it is agnostic toward the origin of a particle trajectory, it is suitable for the reconstruction of secondary tracks from displaced vertices. A new addition to the algorithm is its use of time information of the hits. When spatial information alone is not sufficient anymore for clustering hits into a track, *e.g.* due to event mixing at higher luminosities, the temporal distance can be used to separate hits from different events. The additional computational footprint of this method is minimal, making up approximately 1-2% run-time to a full track reconstruction.

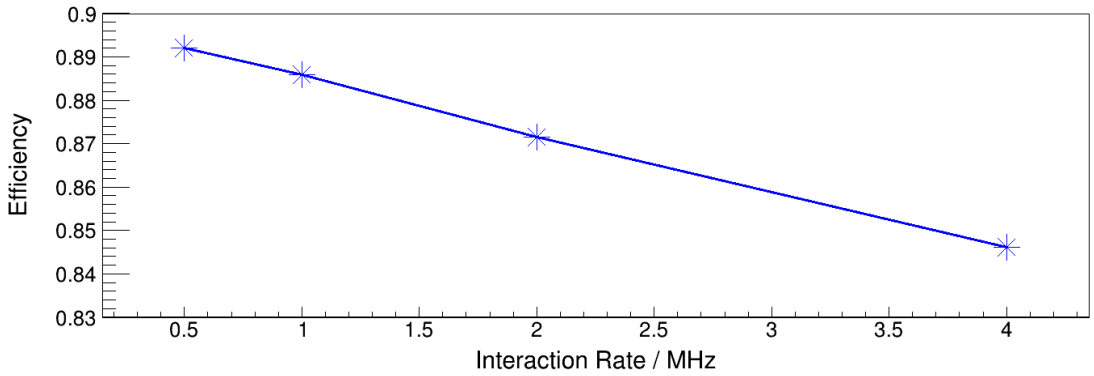

Figure 46: Time-based reconstruction efficiency vs. interaction rate for the SttCellTrackFinder.

Adding a new dimension to the track reconstruction needs to be addressed in the quality assurance (QA) measures, too. Previously, the tracking QA-task in PandaRoot only operated on event-based, but not time-sorted data. The option to run with time-based data has been added to the tracking QA-task, allowing the user to study the various quality observables, *e.g.* momentum resolution, track finding efficiency and purity, under more realistic conditions.

Along this condition, the classifications for found tracks based on these observables have been reworked into:

- Fully purely found: All hits generated from the Monte Carlo track have been found and none have falsely associated.
- Fully impurely found: All hits generated from the Monte Carlo track have been found, but contaminations are present.
- Partially purely found: At least 70% of the hits from the Monte Carlo track have been found and none have been falsely associated.
- Partially impurely found: At least 70% of the hits from the Monte Carlo track have been found, but contaminations are present.

The classifications for ghost and clone track continue to exist alongside these new categories. Fig. 46 shows the reconstruction efficiency of the updated `SttCellTrackFinder` determined with the new tracking QA-task at a range of possible interaction rates. Good efficiencies of 84-89 % have been achieved.

Machine learning continues to show promise for track reconstruction in the Forward Tracking System. Two approaches based on artificial neural networks (ANN) have been implemented. In the *local method*, an ANN is trained to accept hit pair coordinates as input and outputs a probability *P* that the hits belong to the same track. If, for example, *P(hit1,hit2)* and *P(hit2,hit3)* exceed a chosen threshold, then *hit1, hit2,* and *hit3* are assigned to the same track. Two different neural networks are applied to the tracking stations inside the magnetic field and those outside. Afterwards, a Recurrent Neural Networks builds the segments into full tracks.

Graph Neural Networks (GNN) are used for the *global method*. This relatively new class of deep learning architectures can effectively handle irregular data structures, *i.e.* non-Euclidian data. The primary task of the GNN is to associate detector elements by classifying the edges of the graph. The graph is constructed so that the nodes are the recorded hits and the edges are connections between hits in adjacent detector layers. The node features of the input graphs are the hit coordinates, which is illustrated in Fig. 47. The network output, illustrated in Fig. 48, is an edge probability, which is 1 if two hits belong to the same track and 0 otherwise. The probability output can be used in the exact same way as for the *local method.*

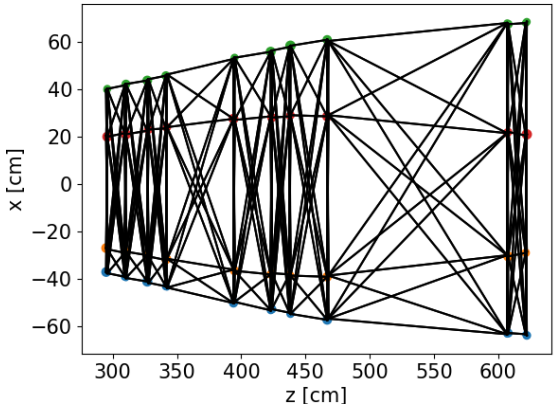

Figure 47: Example input graph, where hit coordinates (colored points) represent node features (x,z). The black lines represent graph edges.

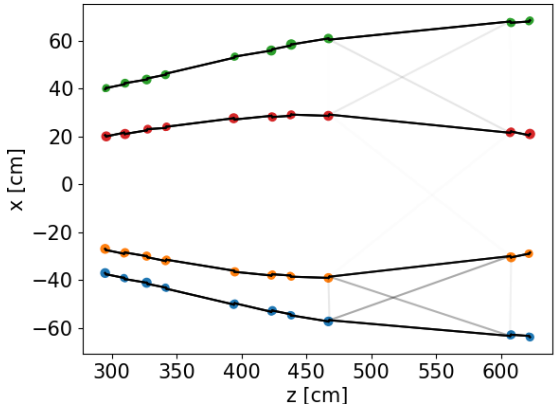

Figure 48: Example output graph. The black lines represent an output probability of 1, while the faded ones represent a number smaller than 1.

Both methods build track projections in the X-Z plane, which only contain hits from the vertical layers. To extend this into three dimensions, the skewed layers in the FTS will be used. The efficiency for both methods is about 75 % for tracks at 1 GeV/*c* and reaches up to 95 % for high

momentum tracks of up to 7 GeV/*c*. The purity ranges from 85-100 % for the local method and is always above 90 % for the global method.

The Electro Magnetic Calorimeter (EMC) of PANDA is the largest and most expensive sub-detector of the experiment. It is essential for all interesting physics channels which include neutral particles. While the R&D phase of the EMC is finished and it is currently under production, the software was missing this maturity for a long time. In the last year it was therefore a major enterprise of several groups to improve the software implementation of the EMC in the PandaRoot software.

The first topic was the digitization of the backward endcap EMC which is an important part of a detailed simulation and gives real detector responses from Monte Carlo hits. Recently, a new digitization algorithm has been developed which has been implement in PandaRoot. A new package has been developed for the backward endcap EMC digitization mainly including a waveform signal generator and waveform parameter extraction. The waveform generator produces waveforms from the Monte Carlo hits including a realistic noise model implementation. The waveform parameter extraction extracts energy and time information from the waveforms including a TMAX filter. The package is fully capable of time-based simulation and by using module separation and common interfaces, the package is flexible and scalable (see Fig. 49). The code development has been finished and has been merged to the 'dev' branch in PandaRoot.

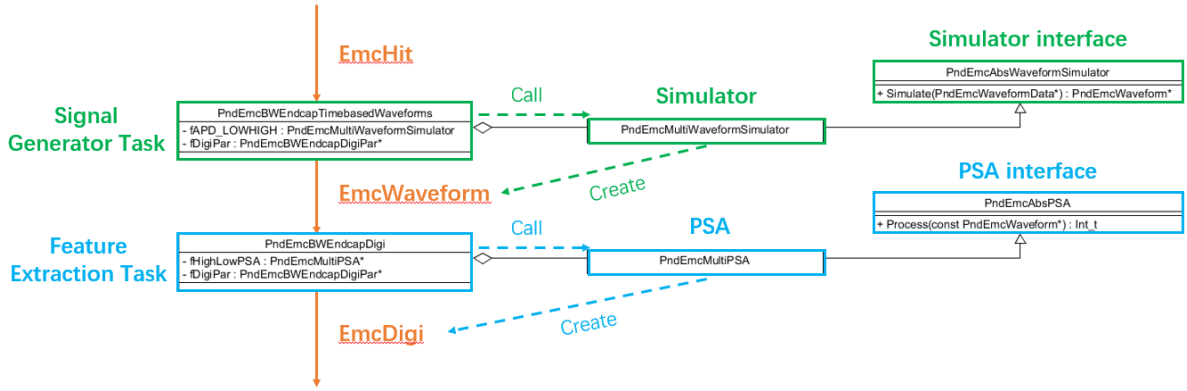

Figure 49: Code structure for the backward endcap EMC digitization

The second topic is the energy and position correction for the EMC as part of the calibration, necessary to improve the resolution of the detector. Preliminary studies on energy/position corrections have been carried out. For the energy correction a two-stage approach was chosen. In the first stage the energies were normalized among crystal types and in the second stage a CMS's method of correction was applied. The result of the two steps can be seen in Fig. 50. For 1 GeV photons the black raw distribution was reconstructed by the software. The red curve shows the change of the distribution by the crystal normalization which makes the peak more narrow but shifts the mean value below its nominal value of 1 GeV while with the second step of the gap correction, originally developed by the CMS experiment, the mean value was shifted to the correct position by keeping the smaller distribution. The methods to correct the position are still under development. Both a traditional log-weighting method and a machine learning method are tried. Furthermore, different methods to perform an EMC calibration have been reviewed and the first based on the usage of pi0 samples was tried.

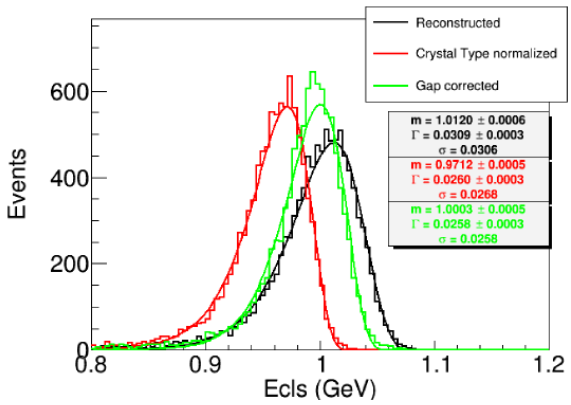

Figure 50: Energy distributions for 1 GeV photon in the EMC. Black histogram is the raw reconstructed energy. Red histogram is the corrected energy of normalizing energies among crystal types. Green histogram is the corrected energy after applying both crystal type correction and the CMS-method correction.

A first version of a new forward endcap geometry for simulation purposes, visible in Fig. 51, was created. It is based on the available forward endcap CAD-model and includes passive material parts such as the insulation, the cooling pipes and the mechanical holding structure. To convert these passive parts a newly developed ROOT-geometry tool `TGeoArbN` was used. This tool allows to convert arbitrary geometry-parts from CAD into simulatable ROOT-geometries using a triangle-mesh representation. With this it was possible to convert for example the cooling pipes depicted in Fig. 51c. The materials implemented for these new parts are currently based on assumptions but will be updated and optimized in the future. Even so, the new geometry and

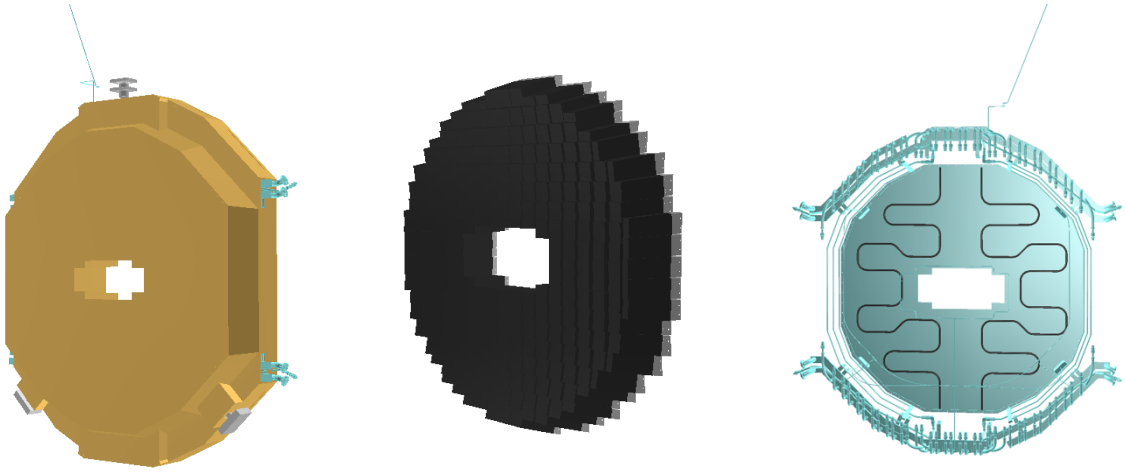

(a) New passive parts including the insulation (golden), the cooling (light blue) and the mechanical holding structure

(b) Alveole assembly hidden by the insulation shown in part (a)

(c) Cooling structure from the back

Figure 51: New forward endcap geometry.

the used materials will allow for more realistic simulations compared to the currently used simulation geometry which does not include the mentioned passive parts.

Integrating the new forward endcap geometry into the simulation proved to be more complicated than expected. Due to historic reasons the subdetectors of the EMC system were treated in software as if they were one entity. This caused code bloat, suboptimal use of the FairRoot provided functionality and also hardcoded geometry combinations. Inserting a new geometry would have meant to add the new geometry to the hardcoded set of combinations which would have required to touch running code in several classes. Therefore, the EMC code for using and including a new geometry in a PandaRoot simulation had to be reworked. The

goal was to allow for easier integration and change of the used detector geometries without touching running code. This restructuring was carried out successfully. However, it became apparent that the overall EMC code required a refactoring. It was considered suboptimal that the EMC code treated all EMC subdetectors (forward and backward endcaps, barrel and shashlik) as a single entity. These four subdetectors shared a single reconstruction chain, making it difficult to specialize the behavior for one specific subdetector. Hence, the reconstruction chain was split into four, one chain for each subdetector.

With this restructuring it was possible also to investigate how much impact the newly created passive parts are on the simulation. Thus, each passive part is included into the simulation as a sensitive detector. This allows to identify all particles that hit the passive parts as well as sum up all the deposited energies. The energy deposited in the cooling structure and its hit map are depicted in Fig. 52 as an example. The pipes visible in Fig. 51c can be distinguished due to a slightly larger entry number in Fig. 52b, as well as the cooling service pipe at theta > 30° protruding the insulation visible in Fig. 51a. More detailed investigations beyond the first glimpse shown here are still to be done.

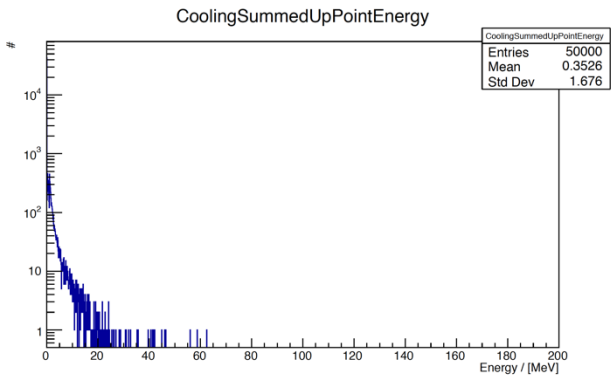

(a) Energy deposited by 50000 randomly shot 2 GeV photons in the cooling structure

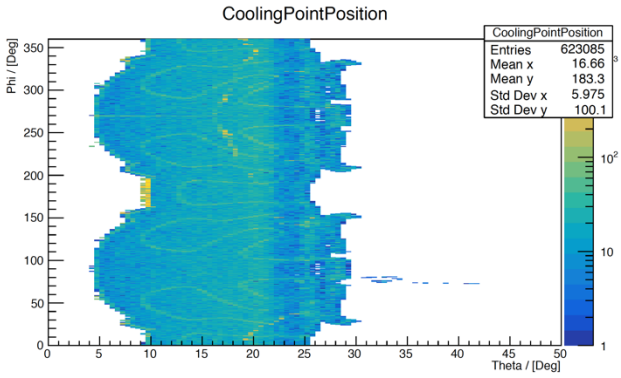

(b) Hit map of Monte Carlo points on the cooling structure. The decrease of entries beyond theta > 22° is due to the overlap with the barrel subdetector.

Figure 52: Cooling structure.

A side effect of using this more detailed geometry created with `TGeoArbN` became apparent in form of an increase of simulation time. First tests seem to indicate that the simulation time may increase substantially. For a simulation of 500 2 GeV photons shot between 5° and 22° in theta the needed time increased by approximately a factor of 2. A generally applicable factor cannot be given so far as the simulation time for the new geometry depends on the level of detail of the triangle meshes used for `TGeoArbN`, the included passive parts and also the used materials. The simulation time is further dependent on the other detectors included in the simulation as well as the energy and the direction of the simulated particles.

A thorough performance study will be needed to be able to decide whether or not the new geometry has to be simplified to be used within a full-scale PANDA simulation. Such a study still has to be done.

Recently additional effort was invested into further separating code that depends on the *offline* available software infrastructure (FairRoot) from code that is responsible for the data processing. This work was started on the one hand to allow reuse of code in the *offline* case and decrease identical, repeated code. On the other hand, it is also planned that certain parts of the data processing code will be used *online*. A first, simple example of using an *offline* algorithm called from *online* like classes (FairMQ) has been developed. This example has proven useful through indicating code shortcomings that will require still further refinement.

During the last year the effort was put in investigateing the time-based simulation for the Forward Endcap EMC (FWEndcap EMC). It was shown that the waveform shape existing in PandaRoot does not correspond to the recent shape obtained from the electronics. In addition, the pile-up recovery procedure existing in PandaRoot was discordant with the one that was implemented on the hardware. Pile-up events are expected to be one of the main issues for the FWEndcap EMC in the Phase-2 of PANDA running in the high luminosity regime, so proper treatment is required also in simulations.

Figure 53: Comparison of waveforms.

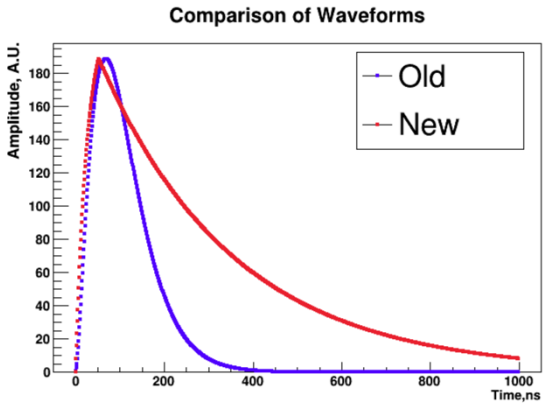

To solve the first problem, the raw measured waveform data was provided, which are produced by the final models of electronics used in the FWEndcap EMC. New shape of waveform and noise characteristics were determined using this data and tested in PandaRoot. The new shape is shown in Fig. 53.

The main discrepancies for the pile-up recovery procedure were an assumption that only two hits can overlap which is not correct and that IIR filters were not used. Therefore, the existing classes `PndEmcPSAFPGAPileupAnalyser` and `PndEmcHighLowPSA` were modified to resolve these discrepancies. Further investigations were focused on optimization of the pile-up recovery procedure by searching for optimal filter parameters. For that studies 10000 photons with an energy of 1 GeV hitting one crystal were simulated at a hit rate of 500 kHz in order to produce pile-up events. The final goal was to estimate the peak energy resolution and the number of reconstructed particles. Fig. 54 shows this peak and its width in sigma.

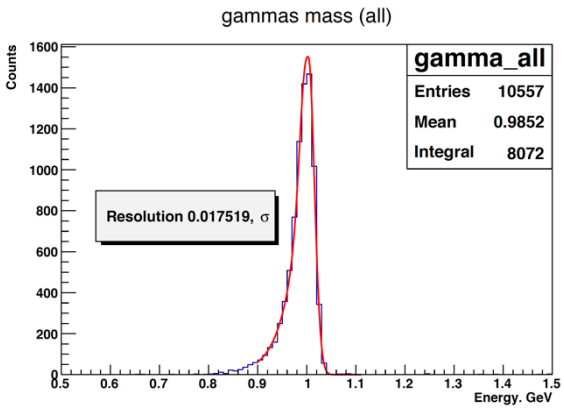

Figure 54: Reconstructed peak of photons

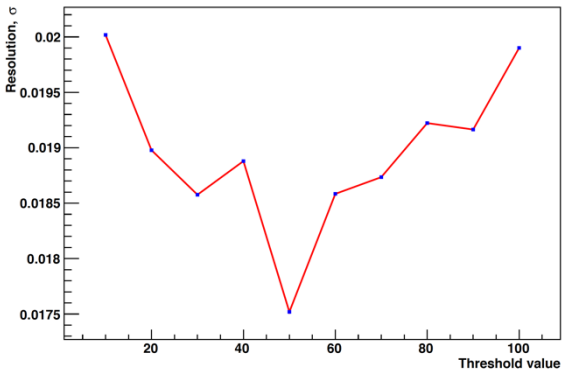

Figure 55: Resolution as a function of the threshold.

The most interesting finding was that an increase of the filter size does not improve the - resolution as it was expected. For that reason, the optimal value of filter the length was found, which is 20 samples for the MWD filter (10 for MA). It was discovered that the final resolution is more sensitive to the threshold values applied during digitization procedure as shown in Fig. 55.

Preparation for Physics

The Standard Model (SM) of particle physics is highly successful in describing the strong interaction at high energies between the fundamental constituents, *i.e.* the quarks and gluons. It still remains a puzzle, however, how these constituents form strongly interacting bound states, the hadrons, with the most prominent, the protons and neutrons, being the building blocks of matter. Similarly, it remains a puzzle to describe the effective interactions among strongly interacting composite objects. The science case of PANDA is to identify the underlying degrees-of-freedom that govern the properties of these complex and dynamic systems on various quantum scales to solve the proton mass millennium problem and understand how 99% of the visible mass of the universe is generated. Furthermore, self-coupling is present in all non-Abelian field theories like gravity, but hadrons are the only place where those effects can be studied in the laboratory. Specifically, PANDA has the ambition to answer the following scientific questions:

- What generates the mass and spin of hadronic matter *e.g.* the proton?
- How are experimental observations related to Quantum Chromodynamics (QCD)?
- What is the reason for the matter-antimatter asymmetry of the universe?
- How does the nuclear force emerge from QCD?
- What is the role of strangeness in *e.g.* neutron stars?
- Where is the limit of stability of hadronic and nuclear matter?

One of the primary objectives of the physics working groups is to sharpen the physics case of PANDA for the first phases of the experiment. Fig. 56 illustrates the four main pillars of PANDA covering the fields of particle, hadron, and nuclear physics. To reach the scientific objectives, various physics channels have been identified in the past to highlight the overall scientific ambitions of PANDA. Monte Carlo (MC) and various reconstruction/analysis techniques, for a large part embedded in PandaROOT, are used to test the feasibility of the foreseen phase-one setup to address the physics goals. A so-called “phase-one paper” is presently under internal review in which the physics capabilities of PANDA in the first phase of the experiment are being reviewed and summarized. In addition, various phase-zero experiments are in preparation and/or (partly) carried out exploiting detector components of PANDA and/or software tools commonly developed with other collaborations. Many of these phase-zero experiments have a strong scientific overlap with the overall ambitions of PANDA as well. Below a summary is given of some of the 2019 activities within each of the four physics pillars.

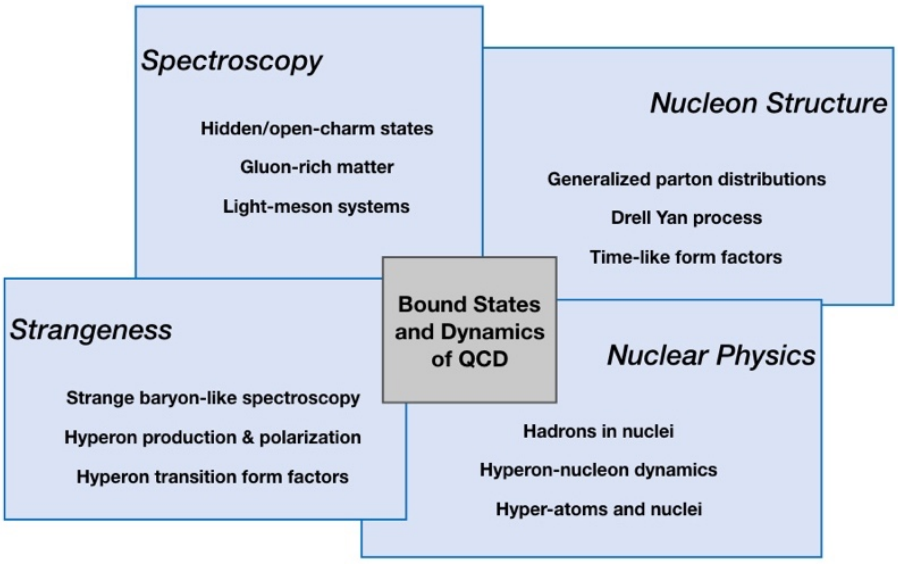

Figure 56: The four scientific pillars of PANDA.

Nucleon structure

The electromagnetic processes (EMP) working group extensively studied the feasibility of identifying the di-lepton channel in antiproton-proton collisions and extracting the form-factors G_E and G_M, and their ratio, at the various phases of PANDA and using both electrons and muons in the final state. In the past year, earlier MC studies were verified using the most up-to-date simulation framework and partly included in the phase-one paper. Moreover, a paper of the di-muon results, based on an earlier approved release note, are in review and close to being submitted to a journal (I. Zimmermann et *al.*). The most recent activities within the EMP community of PANDA include the development of an event generator that accounts for radiative corrections in antiproton-proton annihilations (E. Tomasi-Gustafsson et *al.*), feasibility MC studies of the form factor extraction in the unphysical regime via $\bar{p}p \to \ell^+\ell^-\pi^0$ (A. Dbeyssi et *al.*), and MC studies of Drell-Yan processes for the extraction of TMDs (A. Skachkova et *al.*). Besides measuring form factors in the time-like regime of the proton, PANDA also has the ambition to study the electromagnetic structure of hyperons via their Dalitz transitions (K. Schönning et *al.*). These studies complement the planned phase-zero measurements with HADES of hyperon (Σ(1387), Λ(1405,1520)) radiative transitions produced in proton-proton collisions (W. Esmail et *al.*).

Spectroscopy in the light- and hidden-charm sectors

The charmonium, exotics, and light-meson working group, in particular the GSI-team (K. Götzen et *al.*), published their work on the line-scan studies of the X(3872) as a benchmark study demonstrating the resonance-scanning technique (Eur. Phys. J. A 55, 42, 2019). Various analyses in the XYZ sector are ongoing. In particular, major progress has been made in the MC study of the ϕϕ final-state in $\bar{p}p$ in the search for gluon-rich matter (I. Keshk et *al.*). This channel is considered one of flagship cases for Day-1 within the light-meson and gluonic matter spectroscopy program of PANDA. This because the reaction is known to have a huge cross section in the order of a few microbarns, a factor 100 times larger than expected from the OZI rule, which might hint towards a strong tensor glueball contribution. PANDA is able to study this reaction at energies that go beyond that what has been achieved at LEAR. For the first time, a partial-wave analysis using PAWIAN has been applied in the MC analysis in combination with a resonance scan procedure and using a coupled-channel approach. A release note of this work is in preparation. Other studies include the possibility to study the elusive pentaquark in the strange sector via $\bar{p}p \to \theta^+\bar{\theta}^-$ (D. Veretennikov et *al.*), the feasibility to identify a hidden-charm hybrid state, $\widetilde{\eta_c}$, via the photon-rich final state $\bar{p}p \to \eta\widetilde{\eta_c} \to 7\gamma J/\psi$ and using a genetic algorithm to optimize the signal-to-background ratio (A. Kripko et al.), and many more.

Strangeness, dynamics and baryon spectroscopy

Another flagship for the first phase of PANDA lies in studying the production of antihyperon-hyperon pairs for both |S|=1,2,3 systems near their corresponding production thresholds. Differential cross sections and polarization observables can be measured within a few days for |S|=1,2 whereby the systematic uncertainty will be the limiting factor. The hyperon working group has successfully studied the performance of carrying out the spin analysis in the $\bar{\Lambda}\Lambda$, $\bar{\Xi}\Xi$ (W. Ikegami Andersson et al.), and $\bar{\Lambda}\Sigma$ (G. Perezandrade et *al.*) channels and conducted feasibility studies in the hyperon |S|=2 spectroscopy sector. Moreover, the working group has performed a detailed MC study of the detector signatures and reconstruction methods in hyperon-antihyperon production (J. Regina et *al.*). The work on all these hyperon-antihyperon dynamics studies have been formulated in three internal release notes which have been approved by the collaboration in 2019. The production of hyperon-antihyperon pairs can be extended using a nuclear target. This would allow us to measure the relative asymmetry between the transverse and longitudinal momentum of the two hyperons. These observables are of particular interest since they are sensitive to the antihyperon-nucleus potential. Recent

BUU calculations show excellent perspectives and the results demonstrate that these measurements can be conducted with sufficient statistics in only one week of running at the foreseen luminosity at Day-1 (J. Pochodzalla et *al.*). Next to all these production dynamics studies of baryons with strangeness, MC studies also show promising results in the baryon spectroscopy sector. In particular, PANDA is very suited to study the properties of |S|=2 baryons via, e.g. the reaction $\bar{p}p \rightarrow \Xi^*\bar{\Xi}$, in various final states. Recent MC studies of the decay $\Xi^* \rightarrow \Lambda K$ show very good perspectives and demonstrated the feasibility to determine the spin-parity of the excited baryons using a partial-wave analysis (J. Pütz et al.). A release note describing such an analysis has been approved by the collaboration in 2019. Other studies that were performed last year include the final states $\Xi^* \rightarrow \Xi\pi^+\pi^-$ (A. Lai et *al.*) and $\Xi^* \rightarrow \Xi\pi^0$ (A. Gillitzer et *al.*).

Nuclear physics in SU(3)

The main activities in the nuclear sector are presently concentrated to exploit the role of strange baryons in a nuclear environment motivated by providing key data to unravel the hyperon puzzle in neutron stars. One of the aspects, the production of hyperon-antihyperon pairs in antiproton-nucleus collisions has been addressed above. In general, these activities are in line with the ambition to carry out |S|=2 hypernuclei gamma-spectroscopy experiments using a dedicated setup with PANDA. Although these experiments are not part of the first phase of PANDA, we do foresee to perform a study of hyperatoms already in phase one or two. Simulations have been carried out to demonstrate the gamma spectroscopy capabilities to identify the Ξ^-Pb system (M. Steinen et *al.*). A preliminary study showed that with an efficiency of about 1 %, PANDA will be able to observe more than 10^3 two-X rays+kaon coincidence signals with a sufficient background suppression of $2\text{x}10^6$ in a measurement of 180 days.

All efforts are supported by the Theory Advisory Group (ThAG) which in 2019 comprised the following experts:

Reinhard Alkofer, Gunnar Bali, Nora Brambilla, Stan Brodsky, Umberto D'Alesio, Christian Fischer, Johann Haidenbauer, Christoph Hanhart, Alexei Larionov, Horst Lenske, Stefan Leupold, Anatoli Likhoded, Matthias Lutz, Thomas Mannel, Ulf-G. Meissner, Simone Pacetti, Juan Miguel Nieves Pamplona, Anton Rebhan (since May 2019), Sinead Ryan (chair), Andreas Schaefer, Kirill Semenov-Tian-Shansky, Mark I. Strikman, Eric Swanson, Lech Szymanowski, Rob Timmermans, and Marc Vanderhagen.

Tracking Front-End Developments and Start of Production

In 2010, scientists from the Jagiellonian University (JU) in Cracow were looking for front-end electronics to process signals from straw tubes for the Forward Tracker (FT) detector in the PANDA experiment. The electronics had to be very fast (~1 MHz rate) and in conjunction with the fast electron signal, there is also a slow ion tail component. Existing solutions did not meet the expected requirements. Thus, the group from AGH University of Science and Technology in Cracow started to design a dedicated ASIC (Application Specific Integrated Circuit) for this purpose.

In a short time, the concept of an ASIC with a fast preamplifier and shaper, an ion tail cancellation circuit and a discriminator for Time of Arrival (ToA) measurement was developed. It allowed also a rough measurement of the signal amplitude using the time over threshold technique (TOT). As a next step, the design of a 4-channel prototype ASIC was started in the CMOS AMS 0.35 µm technology and the first prototype was produced. The results of the first tests were very promising. Despite this, the tests were long and tedious, because in the tail cancellation circuit over 4000 settings were possible and had to be optimized in order to obtain the shortest pulse without any tail distortions. Design work and laboratory tests of first prototypes were conducted. Production of prototypes was supported by FZ Jülich, who got also interested in using the ASIC for the readout of Straw Tube Tracker (STT) of PANDA experiment. For the STT the amplitude measurement by means of TOT was investigated in addition to ToA measurement. Long-term tests with radioactive sources and beam-tests conducted at FZ Jülich with first prototypes of FT and STT modules fully confirmed the usefulness of the chip.

Figure 57: Layout of the PASTTREC ASIC.

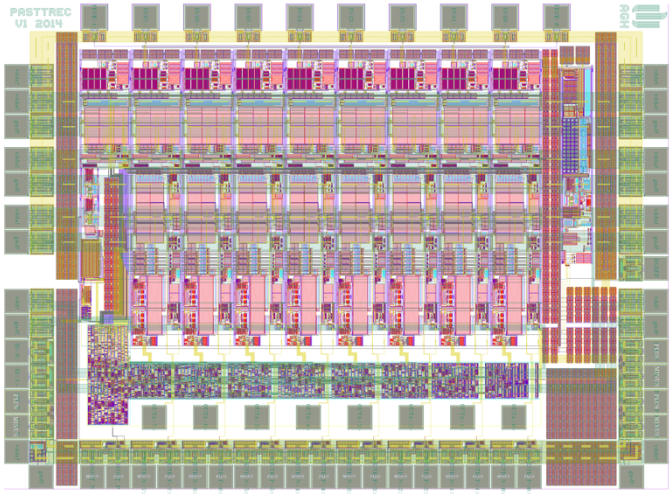

In 2014 an 8-channel improved version of the ASIC called PASTTREC (PAnda STraw Tube REad-out asiC) was designed and fabricated. In PASTTREC, compared to previous version, the core processing blocks have been improved and new functionalities/blocks, such as slow control logic or baseline trimming 5-bit DAC in each channel, have been added. The layout of PASTTREC is shown in Fig. 57 and the photograph of the ASIC in Fig. 58.

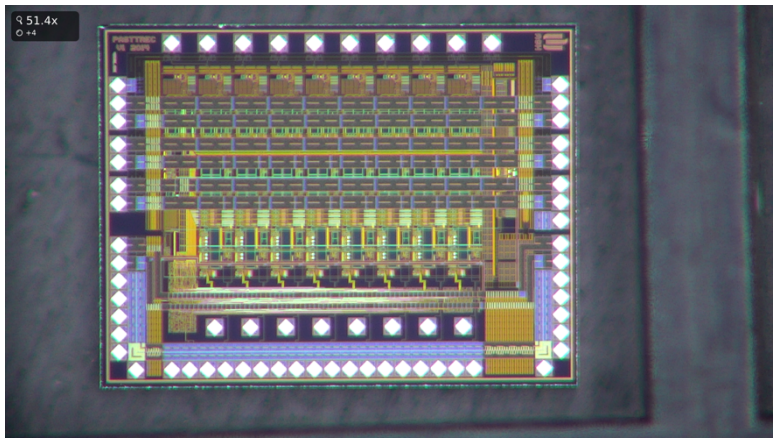

Figure 58: PASTTREC ASIC Die.

Laboratory tests confirmed excellent performance of PASTTREC operation reflected in high speed, low noise and good channel-to-channel uniformity. For the readout of the FT and STT detectors a 16-channel front-end board (two PASTTRECs per board) was developed as shown in Fig. 59. With such front-end boards several beam-tests with setups containing many hundreds of straw tubes were performed to check whether the complete detector system achieves the spatial resolution of 150 µm required by the FT and STT. In addition, for the STT it was studied whether the TOT resolution was sufficient for particle identification, i.e. to separate protons, pions and kaons in a wide momentum range 200 < p < 1000 MeV/*c*. Such range corresponds to the energy deposition in the straw tube in the range between 1-10 MIPs (Minimum Ionizing Particle). The test-beams showed that both the spatial resolution and the energy resolution met the requirements (see Fig. 60). The developed front-end board was accepted as the common solution for both tracking systems.

Figure 59: Front-end board with two PASTTREC ASICs.

In 2019 the In-Kind Contract, regarding the Read-out Electronics for STT and FT in the PANDA Experiment, was signed between the FAIR, JU and AGH. AGH in collaboration with JU will provide the readout electronics for about ~5'000 straw tubes in the STT and for ~15'000 straw tubes in the FT.

Regardless of the future, much has been achieved right now. Very good cooperation was established between AGH and JU in Cracow, under which a complete system for FT tracking consisting from straw tube detector and readout electronics was developed. This cooperation has expanded internationally with FZ Jülich to cover also the readout of the STT detector. The developed PASTTREC-based readout has already resulted in the first spin-offs. This readout has been implemented in the Straw Tube Tracker (STT) detector (~3'000 channels) of the MUSE experiment. Recently, the decision was also made to use the same readout for ~40'000 channels of the Multi-wire Drift Chamber (MDC) detector of the HADES experiment at FAIR.

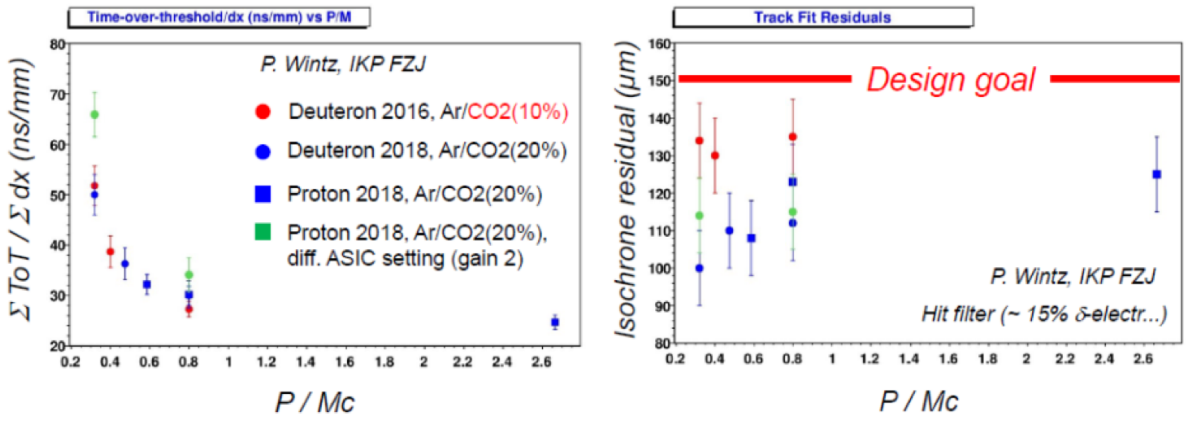

Figure 60: Left: Truncated TOT mean for deuteron and proton measured at different momenta, Right: corresponding spatial resolution.

Study of Excited Ξ Baryons in Antiproton-Proton Collisions

Feasibility studies of Ξ^* resonances decaying into different final states, i.e. $\bar{\Xi}^+\Lambda K^-$ (and $\Xi^-\bar{\Lambda}K^+$ in the charge conjugate), $\bar{\Xi}^+\Xi^-\pi^0$, and $\bar{\Xi}^+\Xi^-\pi^+\pi^-$ have been performed. The results of these studies with main focus on the $\bar{\Xi}^*\Lambda K^-$ and $\Xi\,\Lambda\,K$ final states, including the two resonant states $\Xi(1690)^-$ and $\Xi(1802)^-$ and their charge conjugate, as well as a strategy to determine the spin and parity quantum numbers of specific Ξ^* resonances are discussed.

For the study of the reaction $\bar{p}p \longrightarrow \bar{\Xi}^+\Lambda K^-$ and $\bar{p}p \longrightarrow \Xi^-\bar{\Lambda}K^+$, two analysis strategies have been chosen: One analysis is based on a sequential fit procedure and the other analysis is based on a full decay tree fit. Two data sets containing 10^6 generated events each have been analyzed. For each data set a beam momentum of $p_{\bar{p}}$ = 4.6 GeV/c corresponding to a center-of-mass energy of about 360 MeV above the $\bar{\Xi}^*\Lambda K^-$ and about 100 MeV above the $\Xi^+\Xi(1820)^-$ production threshold has been chosen.

For the analysis using a sequential fit procedure, an ideal PID algorithm was used to select the final state particles. The selection of the composite state particles, namely Λ, $\bar{\Lambda}$, Ξ^- and $\bar{\Xi}^+$, is based on different fits, like a vertex fit and various kinematic fits. The candidates with the highest fit probability are selected for being part of the true signal. All reconstructed candidates are then combined to the $\bar{\Xi}^+\Lambda K^-$ or $\Xi^-\bar{\Lambda}K^+$ (in the charge conjugate channel) final state candidates on which a vertex fit and subsequently a kinematic fit with four-momentum constraint to match the initial four-momentum of the $\bar{p}p$ system is performed. With this analysis strategy a reconstruction efficiency of about 8 % is achieved for the $\bar{\Xi}^+\Lambda K^-$ and of about 9 % for $\Xi^-\bar{\Lambda}K^+$ with a sample purity of 95.4 % each is achieved.

The second analysis uses a full decay tree fit procedure which fits the full decay tree recursively. Different from the other analysis, no Monte Carlo PID information is used for the selection of the final state particles. In this analysis only a mass window cut is applied to the composite state particles to reduce the combinatorial background. Subsequently, the candidate is combined to the $\bar{\Xi}^+\Lambda K^-$ and $\Xi^-\bar{\Lambda}K^+$ system on which the full decay tree fit is performed. The selection results in a reconstruction efficiency of 5.4 % form $\bar{\Xi}^+\Lambda K^-$ and 5.5 % for $\Xi^-\bar{\Lambda}K^+$ and a sample purity of 97.7 % each.

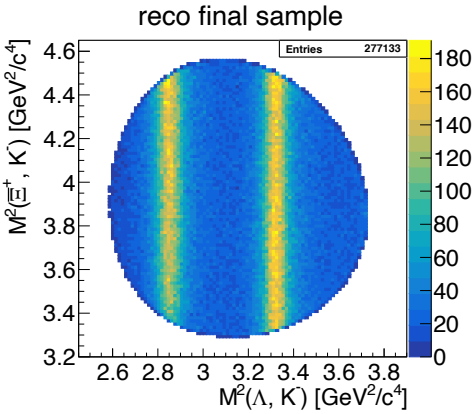

Figure 61: Dalitz plot for the final selected $\bar{\Xi}^+\Lambda K^-$ candidates reconstructed with the full decay tree fit. The Ξ^* resonances are observable as vertical bands.

In addition to the study of the signal events, also a study of the hadronic background has been performed using the same algorithms as for both analyses. In both cases, out of 10^8 generated background events, no event survived the applied cuts. This non- observation of background corresponds on the 90 % confidence to 2.3 events which gives the possibility to calculate a lower limit for the signal-to-background ratio and the signal significance. In case of the full decay tree fit the signal-to-background ratio is estimated to S/B > 19.1 and the signal significance is S_{sig} > 507.

5.6x10^6 events were generated to study the reaction $\bar{p}p \longrightarrow \bar{\Xi}^+\Xi^-\pi^+\pi^-$ and about 9x10^6 events to study $\bar{p}p \longrightarrow \bar{\Xi}^+\Xi^-\pi^0$. Different strategies were used to reconstruct the full decay tree leading to reconstruction efficiencies between 3.9 % and 5.5 % and a sample purity between 97 % and 99 %.

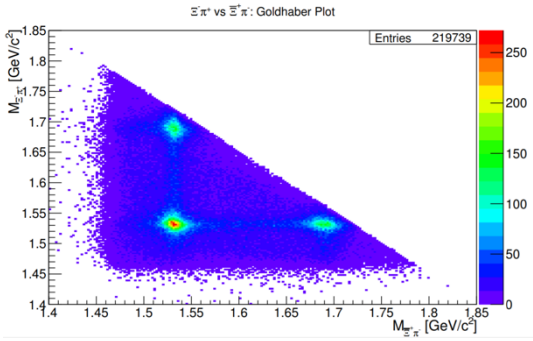

Figure 62: Goldhaber Plot for the final reconstructed neutral Ξπ systems of the reaction $\bar{p}p \longrightarrow \bar{\Xi}^+\Xi^-\pi^+\pi^-$. The vertical bands indicate the neutral Ξ^- resonances.

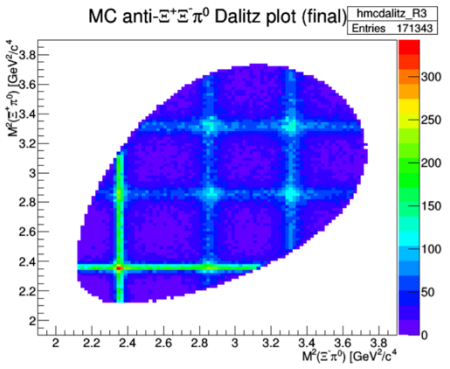

Figure 63: $\bar{\Xi}^+\Xi^-\pi^0$ Dalitz plot for the final selected events of the reaction $\bar{p}p \longrightarrow \bar{\Xi}^+\Xi^-\pi^0$.

Since the spin and parity quantum numbers for most Ξ^* resonances are not known, a feasibility study to determine the quantum number for $\Xi(1690)^-$ and $\Xi(1820)^-$ with PAWIAN is performed. As a first step only the contribution of a single Ξ resonances in each case was investigated. Data sets with different JP -hypotheses, i.e. $1/2^+$, $1/2^-$, $3/2^+$ and $3/2^-$, each, were generated and subsequently fitted with all hypotheses. The preferred fit hypothesis is than evaluated by comparing the BIC and AIC values of the fit results. In addition, data sets also including the reaction $\bar{p}p \longrightarrow \bar{\Lambda}(1890)\,\bar{\Lambda} \longrightarrow \bar{\Xi}^+K^-$ were investigated in the same way.

The study has shown that the determination of the quantum numbers J^P with PAWIAN is possible for the studied simplified cases. Further studies for more generalized cases are ongoing.

Career Development and Completed PhDs in 2019

PANDA PhD Prize 2019

The PANDA PhD Prize 2019 was awarded to Silke Grieser for her work on the "Cluster-Jet Targets for the PANDA-, MAGIX-, and CryoFlash-Experiments at Hadron-, Lepton-, and Laser-Facilities" under the supervision of Alfons Khoukaz from Westfälische Wilhelms-Universität in Münster. The certificate and the prize money of 200€ was presented by the spokesperson during the collaboration Dinner on Nov 6, 2019.

Finished PhD Theses in 2019

- Silke Grieser, U Münster, "Cluster-Jet Targets for the PANDA-, MAGIX-, and Cryoflash Experiments at Hadron-, Lepton-, and Laser-Facilities"
- Alessandra Lai, U Bochum, "Development of a Data Acquisition System for the Custom Front-End Prototypes of the PANDA Micro Vertex Detector and Study of the Reaction pbarp $\rightarrow \Xi^+\Xi^-\pi^+\pi^-$
- Claudius Schnier, RU Bochum, "Analyse des Zerfalls $\eta_c \rightarrow \pi^+\pi^-\eta$ bei BESIII und Entwicklung von Komponenten für das elektromagnetische Kalorimeter des PANDA Experimentes"
- Miriam Kümmel, RU Bochum, "Analysis of $J/\psi \rightarrow \phi\eta\eta$ at BESIII and Calibration of the Temperature Monitoring System for the PANDA Electromagnetic Calorimeter"
- Iris Zimmermann, U Mainz, "Feasibility studies for the measurement of the time-like electromagnetic proton form factors at the PANDA experiment"
- Bertold Fröhlich, U Mainz, "Investigation on intense magnetic flux shielding with a high temperature superconducting tube for a transverse polarized target at the PANDA experiment"
- Benjamin Wohlfahrt, U Giessen, "Matching of Avalanche Photodiodes and Light Injection into Scintillation Crystals"
- Jennifer Pütz, FZ Jülich/U Bochum, "Study of Excited Xi Baryons in Anti-Proton Proton Collisions with the PANDA Detector"
- Tobias Holtmann „Suche nach der $Z_c(3900)^{\pm}$-Resonanz in $e^+e^- \rightarrow p n\pi^-$ + c.c. bei BESIII und Entwicklungen für die Photodetektoren des elektromagnetischen Kalorimeters des PANDA-Experimentes"

Habilitations

- Frank Nerling habilitated at Goethe University Frankfurt on Nov 27, 2019. The title of his thesis is "Exotic Bound States of the Strong Interaction – Experimental Status and Spectroscopy" and the demonstration lesson was about "Cosmic Radiation"

Outstanding Achievement Award 2017-2018

Prizes for outstanding achievements in 2017/18 to the benefit of PANDA have been awarded to three groups at Krabi

Alaa Dbeyssi, Manuel Zambrana, and Iris Zimmermann from the Helmholtz Institute Mainz for their PANDA Physics Achievements Concerning EM Probes

The group has continuously driven the simulations of form factor studies using electromagnetic probes. The group has successfully implemented the formalism to investigate the electromagnetic structure of the proton in the time-like region including the development of radiative corrections and techniques to suppress backgrounds. Their published results were based on detailed Monte Carlo simulations and clearly outlined the capability of PANDA to measure the electric and magnetic form factor at the various phases of the experiment.

Pawel Marciniewski, Filza Saleem, and Peter Schakel from Uppsala University for the Design and Production of the Forward Endcap SADCs

Pawel Marciniewski (Uppsala University) has been responsible for the timely production of the sampling-ADCs for the readout of the forward endcap EM-calorimeter. Through excellent preparation and foresight, they very successfully produced all 250 boards at the Uppsala University. This is an essential component to bring the forward endcap of the EMC into operation during the upcoming tests.

Daniel Bonaventura, Silke Grieser, Benjamin Hetz, and Alfons Khoukaz from University of Münster for the Achievement of World Record Cluster Target Densities

The group has made remarkable achievements with their development of the Cluster Target. By attaining densities of 4×10^{15}/cm for a nozzle over 2m away from the interaction point, they have set a world record and exceeded the PANDA requirements. This excellent target performance will enable a significant rise of the luminosity available at the experiment and thus all physics pillars within PANDA will benefit from it.

- G. Barucca et al., Precision resonance energy scans with the PANDA experiment at FAIR - Sensitivity study for width and line-shape measurements of the X(3872), EPJA Vol. 55, No. 3, 42, 2019, http://arxiv.org/abs/1812.05132
- A. Lehmann et al. (PANDA Cherenkov Group), “Recent progress with microchannel-plate PMTs“, NIMA, in press, https://doi.org/10.1016/j.nima.2019.01.047
- B. Singh et al., The PANDA Collaboration, “Technical Design Report for the PANDA Barrel DIRC Detector”, J. Phys. G: Nucl. Part. Phys. 46 045001, doi:10.1088/1361-6471/aade3d, arXiv:1710.00684
- C. Schwarz et al., The PANDA Cherenkov Group, “The Barrel DIRC detector of PANDA”, Nucl. Instr. and Meth. Phys. Res. Sect. A. (2019), doi:10.1016/j.nima.2018.10.159, arXiv:1901.08432
- E. Etzelmueller et al., The PANDA Cherenkov Group, “The PANDA DIRC Detectors”, Nucl. Instr. and Meth. Phys. Res. Sect. A. (2019), doi:10.1016/j.nima.2019.01.017, arXiv:1901.04283
- M. Schmidt et al., The PANDA Cherenkov Group, “Endcap Disc DIRC for PANDA at FAIR” in: Liu ZA. (eds) Proceedings of International Conference on Technology and Instrumentation in Particle Physics 2017. TIPP 2017. Springer Proceedings in Physics, vol. 212. Springer, Singapore; doi:10.1007/978-981-13-1313-4_52
- M. Düren et al. (PANDA DIRC Group), *Particle Identification with DIRCs at PANDA*, VCI Proceedings, (VCI Proceedings), https://doi.org/10.1016/j.nima.2019.04.068
- A. Lehmann et al. (PANDA DIRC Group), "Latest improvements of microchannel-plate PMTs", VCI2019 Proceedings, https://doi.org/10.1016/j.nima.2019.162357

Talks at Workshops and Conferences in 2019

- Gabriela Pérez Andrade, Talk at 42nd Symposium on Nuclear Physics, *Production of the Sigmabar hyperons in the PANDA experiment at FAIR*, Cocoyoc/Mexico, Jan 7-10, 2019
- Michael Düren, Talk at VCI 2019, *Particle Identification with DIRCs at PANDA*, Vienna/Austria, Feb 18-22, 2019
- Albert Lehmann, Talk at VCI 2019, *Latest Improvements of Microchannel-Plate PMTs*, Vienna/Austria, Feb 18-22, 2019
- Frank Nerling, Talk at From Phi to Psi 2019, *Prospects of charmonium spectroscopy at PANDA/FAIR*, Novosibirsk/Russia, Feb 25-Mar 1, 2019
- Tassos Belias, Talk at ICTP-SAIFR/FAIR Workshop on Mass Generation in QCD, *The PANDA Detector @ FAIR*, Sao Paolo/Brazil, Feb 25-Mar 1, 2019
- Tord Johansson, Talk at ICTP-SAIFR/FAIR Workshop on Mass Generation in QCD, *Prospects of Hyperon Physics with PANDA*, Sao Paolo/Brazil, Feb 25-Mar 1, 2019
- Klaus Peters, Talk at ICTP-SAIFR/FAIR Workshop on Mass Generation in QCD, *XYZ an exotic alphabet for PANDA*, Sao Paolo/Brazil, Feb 25-Mar 1, 2019
- Kai Brinkmann, Talk at ICTP-SAIFR/FAIR Workshop on Mass Generation in QCD, *Photon Spectroscopy at PANDA and Elsewhere*, Sao Paolo/Brazil, Feb 25-Mar 1, 2019
- Tobias Stockmanns, Talk at ICTP-SAIFR/FAIR Workshop on Mass Generation in QCD, *Computing at PANDA*, Sao Paolo/Brazil, Feb 25-Mar 1, 2019
- Jenny Regina, Talk at Connecting the Dots/Intelligent Trackers 2019, *Time based reconstruction of hyperons at PANDA at FAIR*, Valencia/Spain, Apr 2-5, 2019
- Waleed Esmail, Talk at Connecting the Dots/Intelligent Trackers 2019, Machine *Learning for Track Finding at PANDA FTS*, Valencia/Spain, Apr 2-5, 2019
- Markus Preston, Poster at International School of Trigger and Data AcQuisition 2019, *Predicting the Rate of Single Event Upsets in a 28 nm FPGA in the PANDA Experiment*, Surrey/United Kingdom, Apr 3-12, 2019
- Johan Messchendorp, Talk at GHP2019, Denver/United States, *Overview PANDA/BESIII*, Apr 10-12, 2019
- Johan Messchendorp, Talk at the GlueX-PANDA Workshop, *Physics program of PANDA*, Ashburn, May 3-5, 2019
- Tassos Belias, held by Klaus Peters, Talk at the GlueX-PANDA Workshop, *Detector Technologies with PANDA*, Ashburn, May 3-5, 2019
- Tobias Stockmanns, Talks at the GlueX-PANDA Workshop, *PANDA Computing Overview*, Ashburn, May 3-5, 2019
- Ralf Kliemt, Talk at the GlueX-PANDA Workshop, *Machine Learning in PandaRoot*, Ashburn, May 3-5, 2019
- Klaus Götzen, Talk at the GlueX-PANDA Workshop, *Analysis Tools in PandaRoot*, Ashburn, May 3-5, 2019
- Myroslav Kavatsyuk, Talk at New Trend in High-Energy Physics, *The PANDA experiment at FAIR*, Odessa/Ukraine, May 12-18, 2019
- Mustafa Schmidt, Talk at New Trend in High-Energy Physics, *The PANDA Experiment at FAIR (detector overview)*, Odessa/Ukraine, May 12-18, 2019
- Klaus Götzen, Talk at QWG 2019, held by Frank Nerling, *Lineshape Scans with Antiprotons - Solving the X(3872) Puzzle*, Torino/Italy, May 13-17, 2019
- Iman Keshk, Talk at FAIRness 2019, *Precision Resonance Scans at PANDA*, Genova/Italy, May 20-24, 2019
- Walter Ikegami Andersson, Talk at FAIRness 2019, *Future Spin Observables Measurements with the PANDA Detector at FAIR*, Genova/Italy, May 20-24, 2019

- Johan Messchendorp, Talk at MENU2019, *PANDA, the next-generation facility in technology and strong-interaction physics*, Pittsburgh/US, June 2-7, 2019
- Florian Feldbauer, Talk at EPICS Collaboration Meeting, *Deplyoment for the PANDA Detector Control System*, St. Paul-lez-Durance/France, June 2-7, 2019
- Karin Schönning, Talk at NSTAR2019, *Hyperon spectroscopy with PANDA at FAIR*, Bonn/Germany, June 10-14, 2019
- Jennifer Pütz, Talk at NSTAR2019, *Study of $p_{bar}p \rightarrow \Xi_{bar}^{+}\Lambda K^{-}$ with the PANDA Detector, Bonn/Germany*, June 10-14, 2019
- Josef Pochodzalla, Talk at ECT* workshop, *Hyperatoms at PANDA*, Trento/Italy, June 17-21, 2019
- Jochen Schwiening, Talk at Electron-Ion Collider User Meeting, *PANDA: Detector Design & Ongoing R&D Efforts*, Paris/France, July 22-26, 2019
- Mustafa Schmidt, Talk at DPF2019, Boston/USA, *The Innovative Design of the Endcap Disc DIRC for PANDA at FAIR*, July 29-Aug 2, 2019
- Gabriela Perez-Andrade, Talk at Hadron 2019, *Simulation study of the $p_{bar}p \rightarrow \Sigma_{bar}^{0}\Lambda$ reaction with PANDA at FAIR*, Guilin/China, Aug 16-21, 2019
- Georg Schepers, Talk at ICNFP 2019, *The PANDA Experiment at FAIR*, Kolymbari/Greece, Aug 21-30, 2019
- Ilknur Koseoglu-Sari, Talk at ICNFP 2019, *Design of Barrel and Endcap DIRC Detectors for Particle Identification in PANDA*, Kolymbari/Greece, Aug 21-30, 2019
- Magnus Wolke, Talk at 19th Lomonosov Conference, *The PANDA experiment at FAIR*, Moscow/Russia, Aug 22-28, 2019
- Daniela Calvo, Poster at TWEPP 2019, *Study of SEU effects in circuits developed in 110 nm UMC technology*, Santiago de Compostela/Spain, Sep 2-6, 2019
- Karin Schönning, Talk at EFB24, *Invited overview talk: Hyperons - a strange key to the strong interaction*, Guildford/UK, Sep 2-6, 2019
- Malte Albrecht, Lecture at FAIR School 2019, *Lecture on PANDA at FAIR School 2019*, Castiglione della Pescaia/Italy,
  Sep 7-14, 2019
- Sergey Kononov, Talk at DIRC2019, *Forward RICH at PANDA*, Giessen/Germany, Sep 11-13, 2019
- Roman Dzhygadlo, Talk at DIRC2019, *Time imaging reconstruction for the PANDA Barrel DIRC*, Giessen/Germany, Sep 11-13, 2019
- Carsten Schwarz, Talk at DIRC2019, *Status of the PANDA Barrel DIRC Project*, Giessen/Germany, Sep 11-13, 2019
- Ilkunor Koseoglu-Sari, Talk at DIRC2019, *Status of the PANDA Endcap Disc DIRC Project*, Giessen/Germany, Sep 11-13, 2019
- Merlin Böhm, Talk at DIRC2019, *Performance of the most recent MCP-PMTs*, Giessen/Germany, Sep 11-13, 2019
- Karin Schoenning, Talk at the workshop of the Baryon Production at BESIII, *Prospects of baryon physics with PANDA*, Hefei/China, Sep 14-16, 2019
- Markus Moritz, Talk at SCINT 2019, *The PWO-II Electromagnetic Calorimeter for the PANDA Target Spectrometer*, Sendai/Japan, Sep 26-Oct 4, 2019
- Valery Dormenev, Poster at SCINT 2019, *Stimulated Recovery of the Radiation Damage in Lead Tungstate Crystals*, Sendai/Japan, Sep 26-Oct 4, 2019
- Jochen Schwiening, Talk at IEEE 2019, *Recent results from the PANDA DIRC detectors*, Manchester/UK, Oct 26-Nov 2, 2019
- Marcel Steinen, Talk at STRANEX 2019, *Heavy Ξ^{-} hyperatoms at PANDA*, Villazzano/Italy, Oct 21-25, 2019

- Michael Papenbrock, Talk at CHEP 2019, *Track reconstruction with PANDA at FAIR*, Adelaide/Australia, Nov 4-8, 2019
- Roman Dzhygadlo, Talk at CHEP 2019, *Particle identification algorithms for the Panda Barrel DIRC*, Adelaide/Australia, Nov 4-8, 2019
- Malte Albrecht, Lecture at Siam School of High Energy Physics 2019, *Physics for FAIR*, PANDA Lecture, Khanchanaburi/Thailand, Nov 9-14, 2019
- Klaus Peters, Talk at BESIII CM, Overview and Status of FAIR, Beijing/China, Nov 18-22, 2019
- Ralf Kliemt, Talk at BESIII CM, *PANDA Computing*, Beijing/China, Nov 18-22, 2019
- Johan Messchendorp, Talk at BESIII CM, *Physics program of PANDA*, Beijing/China, Nov 18-22, 2019
- Anastasios Belias, Talk at BESIII CM, *PANDA Detector - Overview and Technologies*, Beijing/China, Nov 18-22, 2019
- Marcel Steinen, Talk at Theia-Strong 2020 Workshop, *Heavy Ξ^- hyperatoms at PANDA*, Speyer/Germany, Nov 25-29, 2019
- Johan Messchendorp, Talk at Theia-Strong 2020 Workshop, *Physics with PANDA at Day One*, Speyer/Germany, Nov 25-29, 2019
- Frank Nerling, Talk at 3rd EMMI Workshop on anti-matter, hyper-matter and exotica production at the LHC, *BESIII results and PANDA perspectives*, Wroclaw/Poland, Dec 2-6, 2019

/ This page is intentionally empty /

Frontpage:

Upper half: In clockwise order, starting upper left:

1) Barrel ToF prototypes: railboard PCBs in carbon fibre enclosure

2) PASTREC ASIC for STT/FT readout

3) APD glueing onto PWO crystals

Lower half: In clockwise order, starting upper left:

4) Laser setup in the DIRC Optical Lab at GSI

5) APD screening for the EMC

6) Muon counter prototype at CERN test beam-time

7) GEM 2D Demonstrator

PANDA Annual Report 2019

List of Contents